Available online at www.sciencedirect.com

ScienceDirect

International Journal of Solids and Structures 44 (2007) 2401–2425

INTERNATIONAL JOURNAL OF SOLIDS and STRUCTURES

www.elsevier.com/locate/ijsolstr

Nonlinear analysis and buckling of elastically supported circular shallow arches

Y.-L. Pi *, M.A. Bradford, F. Tin-Loi

School of Civil and Environmental Engineering, The University of New South Wales, Sydney NSW 2052, Australia

Received 17 November 2005; received in revised form 7 July 2006
Available online 21 July 2006

Abstract

Arches are often supported elastically by other structural members. This paper investigates the in-plane nonlinear elastic behaviour and stability of elastically supported shallow circular arches that are subjected to a radial load uniformly distributed around the arch axis. Analytical solutions for the nonlinear behaviour and for the nonlinear buckling load are obtained for shallow arches with equal or unequal elastic supports. It is found that the flexibility of the elastic supports and the shallowness of the arch play important roles in the nonlinear structural response of the arch. The limiting shallownesses that distinguish between the buckling modes are obtained and the relationship of the limiting shallowness with the flexibility of the elastic supports is established, and the critical flexibility of the elastic radial supports is derived. An arch with equal elastic radial supports whose flexibility is larger than the critical value becomes an elastically supported beam curved in elevation, while an arch with one rigid and one elastic radial support whose flexibility is larger than the critical value still behaves as an arch when its shallowness is higher than a limiting shallowness. Comparisons with finite element results demonstrate that the analytical solutions and the values of the critical flexibility of the elastic supports and the limiting shallowness of the arch are valid.

Keywords: Analysis; Asymmetric; Arches; Bifurcation; Buckling; Elastic supports; Nonlinear; Shallow; Snap-through

1. Introduction

The in-plane structural behaviour of a shallow arch (Fig. 1) becomes nonlinear as the external load increases. When the load reaches a certain value, the arch may buckle in a bifurcation mode (Fig. 2(a)) or in a snap-through mode (Fig. 2(b)). Because the deformations of a shallow arch prior to buckling become nonlinear, their effects on the buckling need to be considered. The effects of the prebuckling deformations on the in-plane buckling has been recognized by some researchers (Fung and Kaplan, 1952; Timoshenko and Gere, 1961; Gjelsvik and Bodner, 1962; Schreyer and Masur, 1966; Dickie and Broughton, 1971; Simites, 1976; Kyriakides and Arseculeratne, 1993; Power and Kyriakides, 1994; Pi et al., 2002; Bradford et al., 2002).

* Corresponding author. Tel.: +61 2 93855066; fax: +61 2 93856139.
E-mail address: y.pi@unsw.edu.au (Y.-L. Pi).

0020-7683/$ - see front matter
doi:10.1016/j.ijsolstr.2006.07.011

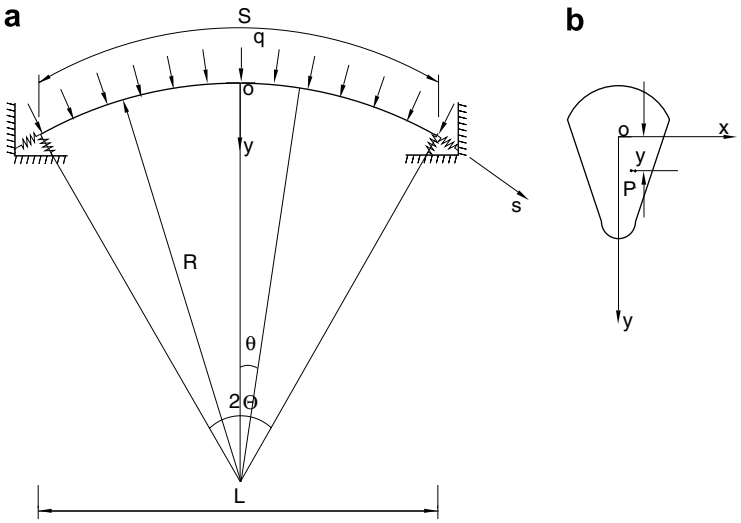

Fig. 1. Arch model. (a) Arch with end restraints and (b) cross-section.

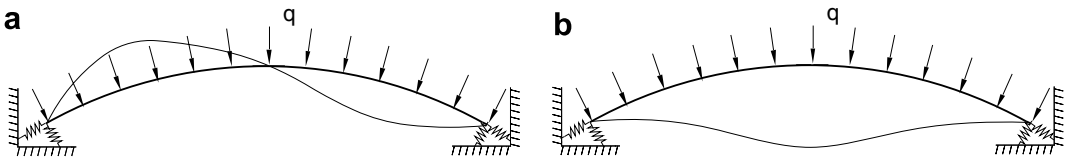

Fig. 2. Buckling modes. (a) Bifurcation buckling and (b) snap-through buckling.

Previous investigations of various shallow arch buckling problems that were analyzed by Fung and Kaplan (1952), Timoshenko and Gere (1961), and Gjelsvik and Bodner (1962) resulted in approximate solutions for various shallow arch buckling problems. Simites (1976) published analytical solutions for sinusoidal shallow arches. Schreyer and Masur (1966) obtained analytical solutions for shallow circular fixed arches (with a rectangular solid section) that are subjected to a uniform radial load or to a central concentrated load. Dickie and Broughton (1971) used a series method to study the buckling of shallow circular pin-ended and fixed arches. However, their study was also confined again to rectangular solid cross-sections and only approximate numerical solutions were given. Dym (1973) studied the bifurcation buckling of pin-ended and fixed arches with rectangular cross-sections and obtained approximate solutions. Kyriakides and Arseculeratne (1993) addressed propagating buckling of long panels with shallow arch cross-sections. Power and Kyriakides (1994) studied the response of long shallow elastic panels to uniform pressure loading. It was demonstrated that their response has the nonlinearity and instability that is characteristic of shallow arches. In addition to a rectangular section, other shapes such as I-sections and hollow sections are used widely for arches. Pi et al. (2002) investigated the in-plane buckling of shallow circular pin-ended and fixed arches with an arbitrary cross-section that are subjected to a uniformly distributed radial load, and obtained closed form solutions, while Bradford et al. (2002) studied in-plane stability of shallow circular pin-ended and fixed arches with an arbitrary cross-section that are subjected to a central concentrated load and obtained analytical solutions. Pi et al. (2002) and Bradford et al. (2002) also obtained the limiting shallowness that determines whether an arch buckles in a snap-through mode or in a bifurcation mode, or for which it does not buckle.

Arches are not necessarily fixed or pin-ended in many cases, but are connected to the adjacent elastic structural elements that provide elastic types of supports to the ends of the arches. The elastically supporting actions of the other elements on an arch can be replaced by equivalent springs. In general, by knowing the structural configuration supporting the arch, the stiffness of the corresponding supports can be estimated. Simply supported arches with ties between their ends are also often used in engineering structures. In this case, the

ties provide an elastic restraint to the arches. It is known that the elastic supports play an important role in the buckling and postbuckling behaviour of structures. The effects of the elastic supports on the buckling of columns and beams have been studied extensively using classical buckling theory (Timoshenko and Gere, 1961; Simites, 1976; Trahair et al., 2001). However, research on the nonlinear behaviour and stability of arbitrarily elastically supported shallow arches does not appear to be reported in the open literature. It is not known how the elastic supports affect the nonlinear behaviour and buckling of shallow arches, nor is the relationship known between the limiting shallowness for determination of buckling modes and the flexibility of the elastic supports. Bradford et al. (2005) and Pi et al. (2006) investigated the nonlinear analysis and buckling of rotationally restrained arches.

The purposes of this paper are: to investigate analytically the in-plane nonlinear elastic behaviour and stability of elastically supported shallow circular arches that are subjected to a radial load uniformly distributed around the arch axis; to obtain analytical solutions for the nonlinear analysis and for the nonlinear buckling load of elastically supported shallow arches; and to derive the relationship between the limiting shallowness of an arch and the flexibility of the elastic supports of the arch.

2. Nonlinear in-plane equilibrium

2.1. Differential equilibrium equations

The nonlinear in-plane equilibrium equations for a shallow elastic arch with elastic supports at both ends and subjected to a radial load uniformly distributed around the arch axis can be obtained from the principle of virtual work that requires

$$\delta V = \int_V E\epsilon\delta\epsilon \,\mathrm{d}V - \int_{-\Theta}^{\Theta} qR^2\delta\tilde{v}\,\mathrm{d}\theta + \sum_{i=\pm\Theta}(k_{v_i}\tilde{v}_i R^2\delta\tilde{v}_i + k_{w_i}\tilde{w}_i R^2\delta\tilde{w}_i) = 0, \tag{1}$$

where V is the volume occupied by the arch, k_{v_i} and k_{w_i} ($i = \pm\Theta$) are the stiffnesses of elastic radial and axial supports at both ends of the arch respectively, $\delta(\,)$ denotes the Lagrange operator of simultaneous variations, ϵ is the longitudinal normal strain at an arbitrary point P at a cross-section, which can be expressed as the sum of the membrane strain ϵ_m and the bending strain ϵ_b as

$$\epsilon = \epsilon_\mathrm{m} + \epsilon_\mathrm{b}, \tag{2}$$

with

$$\epsilon_\mathrm{m} = \tilde{w}' - \tilde{v} + \frac{1}{2}(\tilde{v}')^2 \quad \text{and} \quad \epsilon_\mathrm{b} = -\frac{y\tilde{v}''}{R} \tag{3}$$

where $(\,)' \equiv \mathrm{d}(\,)/\mathrm{d}\theta$ and $(\,)'' \equiv \mathrm{d}^2(\,)/\mathrm{d}\theta^2$, θ is the angular coordinate; $\tilde{v} = v/R$, $\tilde{w} = w/R$, v and w are the radial and axial displacements of the centroid o of the cross-section respectively (as shown in Fig. 1), R is the radius of the initial curvature of the centroidal axis of the arch, and y is the coordinate of the point P in the principal axes.

Substituting Eq. (2) into Eq. (1) and dividing Eq. (1) by the factor EAR leads to the dimensionless form of the virtual work statement

$$\delta V = \int_{-\Theta}^{\Theta}\left[\epsilon_\mathrm{m}(\delta\tilde{w}' - \delta\tilde{v} + \tilde{v}'\delta\tilde{v}') + \frac{r_x^2\tilde{v}''}{R^2}\delta\tilde{v}'' - \frac{qR}{EA}\delta\tilde{v}\right]\mathrm{d}\theta + \sum_{i=\pm\Theta}\left(\frac{k_{v_i}\tilde{v}_i R}{EA}\delta\tilde{v}_i + \frac{k_{w_i}\tilde{w}_i R}{EA}\delta\tilde{w}_i\right) = 0, \tag{4}$$

where $r_x = \sqrt{I_x/A}$ is the radius of gyration of the cross-section about the major principal axis, A is the area of the cross-section.

Integrating Eq. (4) by parts leads to the differential equations of equilibrium

$$\epsilon_\mathrm{m}' = 0 \tag{5}$$

for the axial deformations, and

$$\frac{r_x^2}{R^2}\tilde{v}^{iv} - \epsilon_\mathrm{m} - \epsilon_\mathrm{m}'\tilde{v}' - \epsilon_\mathrm{m}\tilde{v}'' - q\frac{R}{EA} = 0 \tag{6}$$

for the radial deformations; and to the boundary conditions

$$\epsilon_{\mathrm{m}} + \frac{k_{w_\Theta}\tilde{w}R}{EA} = 0 \quad \text{or} \quad \delta\tilde{w} = 0 \qquad \text{at } \theta = \Theta, \tag{7}$$

$$\epsilon_{\mathrm{m}} - \frac{k_{w_{-\Theta}}\tilde{w}R}{EA} = 0 \quad \text{or} \quad \delta\tilde{w} = 0 \qquad \text{at } \theta = -\Theta \tag{8}$$

for the axial direction, and

$$\epsilon_{\mathrm{m}}\tilde{v}' - \frac{r_x^2}{R^2}\tilde{v}''' + \frac{k_{v_\Theta}\tilde{v}R}{EA} = 0 \quad \text{or} \quad \delta v = 0 \qquad \text{at } \theta = \Theta, \tag{9}$$

$$\epsilon_{\mathrm{m}}\tilde{v}' - \frac{r_x^2}{R^2}\tilde{v}''' - \frac{k_{v_{-\Theta}}\tilde{v}R}{EA} = 0 \quad \text{or} \quad \delta v = 0 \qquad \text{at } \theta = -\Theta, \tag{10}$$

$$\tilde{v}'' = 0 \quad \text{or} \quad \delta v' = 0 \qquad \text{at } \theta = \pm\Theta \tag{11}$$

for the radial direction.

From Eq. (5), the membrane strain ϵ_{m} is a constant and can be written as

$$\epsilon_{\mathrm{m}} = -\frac{\overline{N}}{EA}, \tag{12}$$

where $\overline{N}$ is the actual axial compressive force in the arch as distinct from the nominal compressive force qR.

Substituting Eqs. (5) and (12) into Eq. (6) yields

$$\frac{\tilde{v}^{iv}}{\mu^2} + \tilde{v}'' = \bar{q}, \tag{13}$$

where μ is a dimensionless axial force parameter defined by

$$\mu^2 = \frac{\overline{N}R^2}{EI_x}, \tag{14}$$

and $\bar{q}$ is a dimensionless load defined by

$$\bar{q} = \frac{qR - \overline{N}}{\overline{N}} \tag{15}$$

which is a measure of the difference between the nominal axial compressive force qR and the actual axial compressive force $\overline{N}$.

Using the definition of μ in Eq. (14), the membrane strain ϵ_{m} given by Eq. (12) can be rewritten as

$$\epsilon_{\mathrm{m}} = -\frac{\overline{N}}{EA} = -\frac{\mu^2 r_x^2}{R^2}. \tag{16}$$

By substituting Eq. (16), the boundary conditions given by Eqs. (9) and (10) can then be rewritten as

$$-\frac{\mu^2 r_x^2}{R^2}\tilde{v}' - \frac{r_x^2}{R^2}\tilde{v}''' + \frac{k_{v_\Theta}\tilde{v}R}{EA} = 0 \quad \text{or} \quad \delta v = 0 \qquad \text{at } \theta = \Theta \tag{17}$$

and

$$-\frac{\mu^2 r_x^2}{R^2}\tilde{v}' - \frac{r_x^2}{R^2}\tilde{v}''' - \frac{k_{v_{-\Theta}}\tilde{v}R}{EA} = 0 \quad \text{or} \quad \delta v = 0 \qquad \text{at } \theta = -\Theta. \tag{18}$$

2.2. Nonlinear equilibrium equation

The general solution of Eq. (13) can be expressed as

$$\tilde{v} = -\frac{D_1\cos(\mu\theta)}{\mu^2} - \frac{D_2\sin(\mu\theta)}{\mu^2} + D_3\theta + D_4 + \frac{\bar{q}\theta^2}{2}. \tag{19}$$

The boundary conditions given by Eqs. (11), (17) and (18) can be used to determine the coefficients D_1–D_4 as

$$D_1 = -\frac{\bar{q}}{\cos(\mu\Theta)}, \tag{20}$$

$$D_2 = 0, \tag{21}$$

$$D_3 = \frac{(\mu\Theta)^2(\alpha_{v_{-\Theta}} - \alpha_{v_\Theta})\bar{q}\Theta}{(\mu\Theta)^2(\alpha_{v_\Theta} + \alpha_{v_{-\Theta}}) - 1}, \tag{22}$$

$$D_4 = -\frac{\bar{q}}{\mu^2} - \frac{\Theta^2\bar{q}}{2} + \frac{\Theta^2\bar{q}(\mu\Theta)^2[4(\mu\Theta)^2\alpha_{v_\Theta}\alpha_{v_{-\Theta}} - \alpha_{v_\Theta} - \alpha_{v_{-\Theta}}]}{(\mu\Theta)^2(\alpha_{v_\Theta} + \alpha_{v_{-\Theta}}) - 1}, \tag{23}$$

where α_{v_Θ} and $\alpha_{v_{-\Theta}}$ are the ratios of the bending stiffness $4EI_x/S^3$ per unit length of the arch to the stiffnesses k_{v_Θ} and $k_{v_{-\Theta}}$ of the elastic radial supports at $\theta = \pm\Theta$, that are given by

$$\alpha_{v_\Theta} = \frac{4EI_x}{k_{v_\Theta}S^3} \quad \text{and} \quad \alpha_{v_{-\Theta}} = \frac{4EI_x}{k_{v_{-\Theta}}S^3}, \tag{24}$$

which can also be used to measure the flexibilities of the radial supports and so are called the dimensionless flexibilities of the radial supports in the present study. When α_{v_Θ} and/or $\alpha_{v_{-\Theta}}$ vanish, the corresponding radial supports become rigid. The stiffness of the elastic supports depends on the adjacent structural members and the means of connection of the arch ends to the adjacent members. In many cases, both radial elastic supports are symmetric and their stiffnesses are the same, i.e. $\alpha_{v_\Theta} = \alpha_{v_{-\Theta}}$ and so $D_3 = 0$. However, stiffnesses of both radial elastic supports of an arch are not necessarily equal to each other, for example, those of the ends of the side-span arch of multi-span arches.

By substituting Eqs. (20)–(23), the solution given by Eq. (19) can then expressed as

$$\tilde{v} = \frac{\bar{q}}{\mu^2}\left\{\frac{\cos(\mu\theta) - \cos(\mu\Theta)}{\cos(\mu\Theta)} + \frac{1}{2}[(\mu\theta)^2 - (\mu\Theta)^2] - \frac{(\mu\Theta)^3(\alpha_{v_\Theta} - \alpha_{v_{-\Theta}})\mu\theta}{(\mu\Theta)^2(\alpha_{v_\Theta} + \alpha_{v_{-\Theta}}) - 1} + \frac{(\mu\Theta)^4[4(\mu\Theta)^2\alpha_{v_\Theta}\alpha_{v_{-\Theta}} - \alpha_{v_\Theta} - \alpha_{v_{-\Theta}}]}{(\mu\Theta)^2(\alpha_{v_\Theta} + \alpha_{v_{-\Theta}}) - 1}\right\}, \tag{25}$$

which describes the nonlinear relationship of the dimensionless radial displacement $\tilde{v}$ with the axial force parameter μ and the dimensionless load $\bar{q}$, and consequently the relationship of $\tilde{v}$ with the actual axial force $\overline{N}$ and the external load $\bar{q}$.

The nonlinear equilibrium equation between the dimensionless load $\bar{q}$ and the modified axial force parameter $\mu\Theta$, and consequently between $\bar{q}$ and the actual axial load $\overline{N}$, can be established by considering that the constant membrane strain given by Eq. (12) should be equal to the average membrane strain over the arch calculated from Eq. (3), so that

$$\epsilon_m = -\frac{\overline{N}}{EA} = \frac{1}{2\Theta}\int_{-\Theta}^{\Theta}\left(\tilde{w}' - \tilde{v} + \frac{\tilde{v}'^2}{2}\right)\mathrm{d}\theta. \tag{26}$$

From the boundary conditions in the axial direction given by Eqs. (7) and (8), the axial dimensionless displacements $\tilde{w}_{-\Theta}$ and $\tilde{w}_\Theta$ at both ends of the arch can be expressed as

$$\tilde{w}_\Theta = -\frac{\epsilon_m EA}{k_{w_\Theta}R} \quad \text{and} \quad -\tilde{w}_{-\Theta} = -\frac{\epsilon_m EA}{k_{w_{-\Theta}}R}. \tag{27}$$

Hence, by considering Eq. (16), the first term of the right hand side of Eq. (26) becomes

$$\frac{1}{2\Theta}\int_{-\Theta}^{\Theta}\tilde{w}'\,\mathrm{d}\theta = \tilde{w}_\Theta - \tilde{w}_{-\Theta} = \frac{\mu^2 r_x^2}{R^2}\left(\frac{EA}{k_{w_\Theta}S} + \frac{EA}{k_{w_{-\Theta}}S}\right) = (\alpha_{w_\Theta} + \alpha_{w_{-\Theta}})\frac{\mu^2 r_x^2}{R^2}, \tag{28}$$

where α_{w_Θ} and $\alpha_{w_{-\Theta}}$ are the ratios of the axial stiffness EA/S per unit length of the arch to the stiffnesses k_{w_Θ} and $k_{w_{-\Theta}}$ of the elastic axial supports and defined by

$$\alpha_{w_\Theta} = \frac{EA}{k_{w_\Theta}S} \quad \text{and} \quad \alpha_{w_{-\Theta}} = \frac{EA}{k_{w_{-\Theta}}S}, \tag{29}$$

which can also be used to measure the flexibilities of the axial supports and so are called the dimensionless flexibilities of the axial supports in the present study. When α_{w_Θ} and/or $\alpha_{w_{-\Theta}}$ vanish, the corresponding axial supports become rigid.

Substituting Eqs. (25), (27) and (28) into Eq. (26) and then integrating leads to the nonlinear transcendental equilibrium equation as

$$A_1\bar{q}^2 + B_1\bar{q} + C_1 = 0, \tag{30}$$

where

$$A_1 = \frac{1}{4(\mu\Theta)^2}\left[5 - \frac{5\tan(\mu\Theta)}{\mu\Theta} + \tan^2(\mu\Theta)\right] + \frac{1}{6} + \frac{\mu^4\Theta^4(\alpha_{v_\Theta} - \alpha_{v_{-\Theta}})^2}{2[(\mu\Theta)^2(\alpha_{v_\Theta} + \alpha_{v_{-\Theta}}) - 1]^2}, \tag{31}$$

$$B_1 = \frac{1}{(\mu\Theta)^2}\left[1 - \frac{\tan(\mu\Theta)}{\mu\Theta}\right] + \frac{1}{3} - \frac{(\mu\Theta)^2[4(\mu\Theta)^2\alpha_{v_\Theta}\alpha_{v_{-\Theta}} - \alpha_{v_\Theta} - \alpha_{v_{-\Theta}}]}{(\mu\Theta)^2(\alpha_{v_\Theta} + \alpha_{v_{-\Theta}}) - 1}, \tag{32}$$

$$C_1 = \left(\frac{\mu\Theta}{\lambda}\right)^2(1 + \alpha_{w_\Theta} + \alpha_{w_{-\Theta}}), \tag{33}$$

in which λ is the shallowness for an arch defined by

$$\lambda = \frac{R\Theta^2}{r_x} = \frac{S^2}{4r_xR}. \tag{34}$$

The shallowness λ of an arch is an important parameter that governs the nonlinear behaviour of the arch. When the shallowness λ is sufficiently small, the shallow arch does not snap-through and its behaviour is similar to a beam curved in elevation.

Eq. (30) describes the nonlinear relationship between the dimensionless load $\bar{q}$ and the axial force parameter μ, and consequently between $\bar{q}$ and the actual axial force $\overline{N}$. The typical nonlinear behaviour of arches with elastic radial supports are shown in Fig. 3(a) and (c) as variations of the dimensionless external load qR/N_{EA} with the dimensionless central radial displacement v_c/f, and in Fig. 3(b) and (d) as variations of the dimensionless

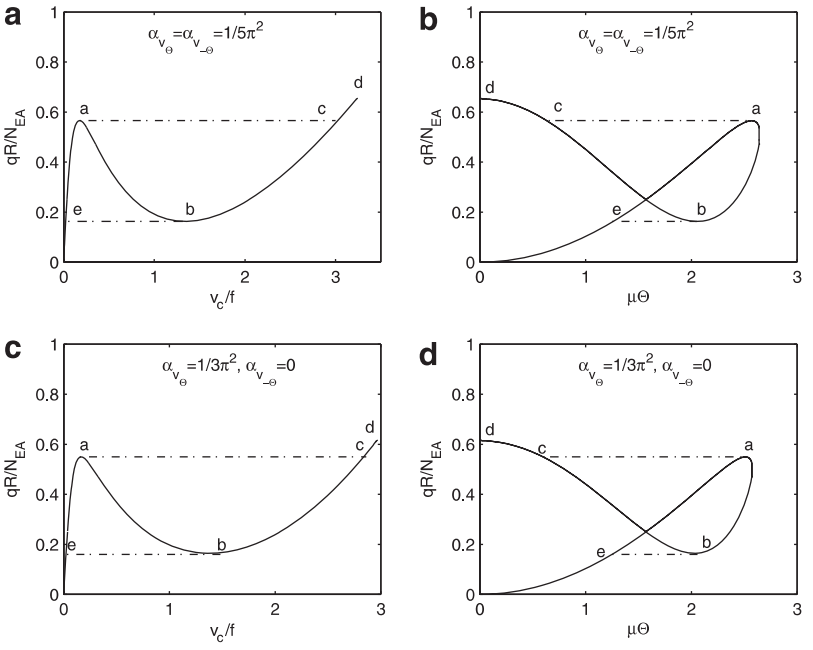

Fig. 3. Nonlinear behaviour of an elastically supported arch.

external load qR/N_{EA} with the modified axial force parameter $\mu\Theta$, where f is the rise of the arch and N_{EA} is the second mode flexural buckling load of the corresponding pin-ended column given by

$$N_{EA} = \frac{\pi^2 EI_x}{(S/2)^2}. \tag{35}$$

The arch in Fig. 3(a) and (b) has equal elastic radial supports of flexibility $\alpha_{v_\Theta} = \alpha_{v_{-\Theta}} = 1/5\pi^2$ at both ends, while the arch in Fig. 3(c) and (d) has one rigid and one elastic radial support (flexibility $\alpha_{v_\Theta} = 1/3\pi^2$). For convenience, the axial supports are assumed to be rigid for arches in Fig. 3.

It can be seen from Fig. 3 that the structural behaviour of the arches become nonlinear even when the load is small. Under displacement control, as the displacement v_c/f increases, the axial force parameter $\mu\Theta$ and the external load qR/N_{EA} increase along the equilibrium path $0a$ until the maximum limit point a is reached. Further increase of the displacement v_c/f is associated with a decrease of the axial force parameter $\mu\Theta$ and of the external load qR/N_{EA} along the path ab until the minimum limit point b is reached. After that, as the displacement continues to increase, and the axial force parameter and the external load increase again along the equilibrium path bd.

3. Buckling analysis

3.1. Snap-through buckling

When the arch shown in Fig. 3 is loaded in a load-controlled manner, as the load increases, the stable equilibrium path $0a$ is first followed, until the limit point a is reached. When the load is further increased by an infinitesimal amount above the limit value, there is no adjacent equilibrium configuration and the only possible equilibrium state is a finite distance apart, i.e. at the state corresponding to the point c as shown in Fig. 3. Therefore, the arch snaps through from equilibrium point a to equilibrium point c, as indicated by the dashed lines in Fig. 3, which are not equilibrium paths. When the external load decreases, the arch follows the path dcb until a limit state corresponding to the point b is reached. If the load is further decreased by an infinitesimal amount, there is no adjacent equilibrium state and the arch will snap-through to the equilibrium state corresponding to point e. The loads corresponding to the limit points a and b are called the snap-through buckling loads. From Eqs. (15) and (30), the load q can be expressed as an implicit function of the dimensionless axial force parameter μ as $F(q,\mu) = 0$. Because the snap-through buckling load q corresponds to limit points a and b, the snap-through buckling load can be obtained by setting

$$\frac{\mathrm{d}q}{\mathrm{d}\mu} = 0, \tag{36}$$

which leads to the equilibrium equation for snap-through buckling load $\bar{q}_{\mathrm{st}}$ as

$$A_2\bar{q}_{\mathrm{st}}^2 + B_2\bar{q}_{\mathrm{st}} + C_2 = 0, \tag{37}$$

where

$$A_2 = 2A_1 + D_2, \tag{38}$$

$$B_2 = 4A_1, \tag{39}$$

$$C_2 = B_1 - C_1, \tag{40}$$

with

$$D_2 = \frac{15}{8\mu^2\Theta^2} - \frac{15\tan(\mu\Theta)}{8\mu^3\Theta^3} - \frac{\tan(\mu\Theta)}{4\mu\Theta} - \frac{\tan(\mu\Theta)^3}{4\mu\Theta} + \frac{7\tan(\mu\Theta)^2}{8\mu^2\Theta^2} + \frac{\mu^4\Theta^4(\alpha_{v_\Theta} - \alpha_{v_{-\Theta}})^2}{[\mu^2\Theta^2(\alpha_{v_\Theta} + \alpha_{v_{-\Theta}}) - 1]^3}. \tag{41}$$

The snap-through buckling load $\bar{q}_{\mathrm{st}}$ of an arch and the corresponding axial force parameter μ can be obtained by solving Eqs. (30) and (37) for a given arch simultaneously, whose shallowness λ, included angle Θ, and flexibilities α_{v_Θ}, $\alpha_{v_{-\Theta}}$, α_{w_Θ}, and $\alpha_{w_{-\Theta}}$ of the elastic supports are known. Once the axial force parameter μ is obtained, the actual axial force $\overline{N}$ and the displacement $\tilde{v}$ corresponding to the snap-through buckling can be

calculated from Eqs. (14) and (25), respectively. It is worth pointing out that if the arch is too shallow, it does not snap-though. The limiting shallowness λ_{sn} that defines a switch between snap-through buckling and no buckling will be discussed in Section 3.6.

3.2. Differential equations of buckling equilibrium

The snap-through buckling Eq. (37) can also be obtained by considering buckling equilibrium. It is assumed that a prebuckling equilibrium configuration is defined by $\{\tilde{v},\tilde{w}\}$ while a buckled equilibrium configuration is defined by $\{\tilde{v}^*=\tilde{v}+\tilde{v}_b,\ \tilde{w}^*=\tilde{w}+\tilde{w}_b\}$ where $\tilde{v}^*$ and $\tilde{w}^*$ are the infinitesimally close to the prebuckled state $\{\tilde{v},\tilde{w}\}$ and so $\tilde{v}_b$ and $\tilde{w}_b$ are infinitesimal buckling displacements in the radial and axial directions respectively. Because a buckled state is an equilibrium configuration infinitesimally adjacent to the prebuckling configuration, the virtual work principle holds for all the admissible virtual displacements $\delta\tilde{v}_b$ and $\delta\tilde{w}_b$ from the buckled equilibrium configuration and can be stated as

$$\delta V^*=\int_V E\epsilon^*\delta\epsilon_b\,dV-\int_{-\Theta}^{\Theta}qR^2\delta\tilde{v}_b\,d\theta+\sum_{i=\pm\Theta}(k_{v_i}\tilde{v}_{ib}R^2\delta\tilde{v}_{ib}+k_{w_i}\tilde{w}_{ib}R^2\delta\tilde{w}_{ib})=0, \tag{42}$$

where the strain ϵ^* consists of the membrane strain ϵ^*_m and the bending strain ϵ^*_{bn} as

$$\epsilon^*=\epsilon^*_m+\epsilon^*_{bn} \tag{43}$$

with

$$\epsilon^*_m=\tilde{w}^{*\prime}-\tilde{v}^*+\frac{1}{2}(\tilde{v}^{*\prime})^2\quad\text{and}\quad\epsilon^*_{bn}=-\frac{y\tilde{v}^{*\prime\prime}}{R}, \tag{44}$$

and the virtual strain $\delta\epsilon_b$ due to the virtual displacements $\delta\tilde{v}_b$ and $\delta\tilde{w}_b$ is given by

$$\delta\epsilon_b=\delta\tilde{w}_b'-\delta\tilde{v}_b+(\tilde{v}'+\tilde{v}_b')\delta\tilde{v}_b'. \tag{45}$$

Substituting Eq. (43) into Eq. (42) leads to the expression for the virtual work statement in the buckled configuration given by

$$\begin{aligned}\delta V^*=&\int_{-\Theta}^{\Theta}\left\{\epsilon^*_m[\delta\tilde{w}_b'-\delta\tilde{v}_b+(\tilde{v}'+\tilde{v}_b')\delta\tilde{v}_b']+\frac{r_x^2(\tilde{v}''+\tilde{v}_b'')}{R^2}\delta\tilde{v}_b''-\frac{qR}{EA}\delta\tilde{v}_b\right\}d\theta\\&+\sum_{i=\pm\Theta}\left[\frac{k_{v_i}(\tilde{v}+\tilde{v}_b)_iR}{EA}\delta\tilde{v}_{ib}+\frac{k_{w_i}(\tilde{w}+\tilde{w}_b)_iR}{EA}\delta\tilde{w}_{ib}\right]=0.\end{aligned}$$

Integrating Eq. (46) by parts leads to the differential equations of equilibrium

$$\{\epsilon^*_m\}'=0 \tag{47}$$

for the axial deformations, and

$$\frac{r_x^2}{R^2}(\tilde{v}^{iv}+\tilde{v}_b^{iv})-\epsilon^*_m-\epsilon^{*\prime}_m(\tilde{v}'+\tilde{v}_b')-\epsilon^*_m(\tilde{v}''+\tilde{v}_b'')-q\frac{R}{EA}=0 \tag{48}$$

for radial deformations; and to the boundary conditions

$$\epsilon^*_m+\frac{k_{w_\Theta}\tilde{w}^*R}{EA}=0\quad\text{or}\quad\delta\tilde{w}_b=0\qquad\text{at }\theta=\Theta, \tag{49}$$

$$\epsilon^*_m-\frac{k_{w_{-\Theta}}\tilde{w}^*R}{EA}=0\quad\text{or}\quad\delta\tilde{w}_b=0\qquad\text{at }\theta=-\Theta \tag{50}$$

for the axial direction, and

$$-\frac{\mu^2r_x^2}{R^2}\tilde{v}^{*\prime}-\frac{r_x^2}{R^2}\tilde{v}^{*\prime\prime\prime}+\frac{k_{v_\Theta}\tilde{v}^*R}{EA}=0\quad\text{or}\quad\delta\tilde{v}_b=0\quad\text{at }\theta=\Theta, \tag{51}$$

$$-\frac{\mu^2r_x^2}{R^2}\tilde{v}^{*\prime}-\frac{r_x^2}{R^2}\tilde{v}^{*\prime\prime\prime}-\frac{k_{v_{-\Theta}}\tilde{v}^*R}{EA}=0\quad\text{or}\quad\delta\tilde{v}_b=0\quad\text{at }\theta=-\Theta, \tag{52}$$

$$\tilde{v}^{*\prime\prime}=0\quad\text{or}\quad\delta\tilde{v}_b^{*\prime}=0\quad\text{at }\theta=\pm\Theta \tag{53}$$

for the radial direction.

From Eq. (47), the membrane strain $\epsilon_{\mathrm{m}}^{*}$ in the buckled configuration is a constant and can be written as

$$\epsilon_{\mathrm{m}}^{*} = -\frac{\overline{N}^{*}}{EA}, \tag{54}$$

where $\overline{N}^{*}$ is the actual axial compressive force in the arch in the buckled configuration.

The virtual work principle arising from virtual displacements $\delta\tilde{v}_{\mathrm{b}}$ and $\delta\tilde{w}_{\mathrm{b}}$ also holds for the equilibrium configuration prior to buckling defined by $(\tilde{v}, \tilde{w})$, which leads to the differential equations of equilibrium given by Eqs. (5) and (6), and the corresponding boundary conditions given by Eqs. (7)–(10). The differential equation of buckling equilibrium for axial deformations can then be obtained by substituting Eq. (5) into Eq. (47) as

$$(\epsilon_{\mathrm{mb}})' = 0, \tag{55}$$

while the differential equation of buckling equilibrium for radial deformations can be obtained by substituting Eqs. (6), (47) and (54) into Eq. (48) as

$$\frac{\tilde{v}_{\mathrm{b}}^{iv}}{\mu^2} + \tilde{v}_{\mathrm{b}}'' = \frac{R^2\epsilon_{\mathrm{mb}}}{r_x^2\mu^2}(1 + \tilde{v}''), \tag{56}$$

where

$$\epsilon_{\mathrm{mb}} = \epsilon_{\mathrm{m}}^{*} - \epsilon_{\mathrm{m}} = \tilde{v}_{\mathrm{b}}' - \tilde{v}_{\mathrm{b}} + \tilde{v}'\tilde{v}_{\mathrm{b}}' \tag{57}$$

is the membrane strain due to buckling displacements.

The corresponding boundary conditions for the buckling equilibrium can also be obtained by substituting Eqs. (7)–(10) into Eqs. (49)–(53) respectively as

$$\epsilon_{\mathrm{mb}} + \frac{k_{w_\Theta}\tilde{w}_{\mathrm{b}}R}{EA} = 0 \quad \text{at } \theta = \Theta, \tag{58}$$

$$\epsilon_{\mathrm{mb}} - \frac{k_{w_{-\Theta}}\tilde{w}_{\mathrm{b}}R}{EA} = 0 \quad \text{at } \theta = -\Theta, \tag{59}$$

for the axial direction, and

$$-\frac{\mu^2 r_x^2}{R^2}\tilde{v}_{\mathrm{b}}' - \frac{r_x^2}{R^2}\tilde{v}_{\mathrm{b}}''' + \frac{k_{v_\Theta}R\tilde{v}_{\mathrm{b}}}{EA} = 0 \quad \text{at } \theta = \Theta, \tag{60}$$

$$-\frac{\mu^2 r_x^2}{R^2}\tilde{v}_{\mathrm{b}}' - \frac{r_x^2}{R^2}\tilde{v}_{\mathrm{b}}''' - \frac{k_{v_{-\Theta}}R\tilde{v}_{\mathrm{b}}}{EA} = 0 \quad \text{at } \theta = -\Theta, \tag{61}$$

$$\tilde{v}_{\mathrm{b}}'' = 0 \quad \text{at } \theta = \pm\Theta \tag{62}$$

for the radial direction.

From Eq. (55), the membrane strain ϵ_{mb} during buckling is a constant. Eq. (37) for snap-through buckling can be obtained by considering the average membrane strain over the length of the arch from Eq. (57) is equal to the constant membrane strain as

$$\frac{1}{2\Theta}\int_{-\Theta}^{\Theta}(\tilde{v}_{\mathrm{b}}' - \tilde{v}_{\mathrm{b}} + \tilde{v}'\tilde{v}_{\mathrm{b}}')\,\mathrm{d}\theta = \epsilon_{\mathrm{mb}} \tag{63}$$

which leads to Eq. (37).

3.3. Bifurcation buckling equilibrium

In addition to snap-through buckling, an elastically supported arch may also buckle in a bifurcation mode. Bifurcation buckling is an adjacent deformation which is characterized by the fact that, as the load passes through its critical stage, the arch passes from its unbuckled equilibrium configuration to an infinitesimally close buckled equilibrium configuration. During bifurcation buckling, both the external loads and internal stress resultants are constant, so that the axial compressive force $\overline{N}^{*}$ in the buckled configuration is equal

to the axial compressive force $\overline{N}$ in the prebuckled configuration. Hence, the membrane strain in the buckled configuration given by Eq. (54) can be written as

$$\epsilon_{\mathrm{m}}^{*} = -\frac{\overline{N}^{*}}{EA} = -\frac{\overline{N}}{EA}. \tag{64}$$

The membrane strain ϵ_{mb} due to buckling deformations can then be obtained by substituting Eqs. (12) and (64) into Eq. (57) as

$$\epsilon_{\mathrm{mb}} = \epsilon_{\mathrm{m}}^{*} - \epsilon_{\mathrm{m}} = -\frac{\overline{N}}{EA} + \left(-\frac{\overline{N}}{EA}\right) = 0. \tag{65}$$

Substituting $\epsilon_{\mathrm{mb}} = 0$ into Eq. (56) leads to the linear homogeneous differential equation for bifurcation buckling of shallow arches as

$$\frac{\tilde{v}_{\mathrm{b}}^{iv}}{\mu^2} + \tilde{v}_{\mathrm{b}}'' = 0. \tag{66}$$

The general solution of Eq. (66) can be written as

$$\tilde{v}_{\mathrm{b}} = E_1\cos(\mu\theta) + E_2\sin(\mu\theta) + E_3\theta + E_4, \tag{67}$$

where E_1–E_4 are coefficients.

The use of the boundary conditions given by Eqs. (60)–(62) leads to the following four linear homogeneous algebraic equations:

$$\cos(\mu\Theta)E_1 + \sin(\mu\Theta)E_2 + \Theta(1 - 2\mu^2\Theta^2\alpha_{v_\Theta})E_3 + E_4 = 0, \tag{68}$$

$$-\cos(\mu\Theta)E_1 + \sin(\mu\Theta)E_2 + \Theta(1 - 2\mu^2\Theta^2\alpha_{v_{-\Theta}})E_3 - E_4 = 0, \tag{69}$$

$$-\mu^2\cos(\mu\Theta)E_1 - \mu^2\sin(\mu\Theta)E_2 = 0, \tag{70}$$

$$-\mu^2\cos(\mu\Theta)E_1 + \mu^2\sin(\mu\Theta)E_2 = 0. \tag{71}$$

The requirement of the existence of nontrivial solutions for E_1–E_4 leads to the vanishing of the determinant

$$\begin{vmatrix} \cos(\mu\Theta) & \sin(\mu\Theta) & \Theta(1 - 2\mu^2\Theta^2\alpha_{v_\Theta}) & 1 \\ -\cos(\mu\Theta) & \sin(\mu\Theta) & \Theta(1 - 2\mu^2\Theta^2\alpha_{v_{-\Theta}}) & -1 \\ -\mu^2\cos(\mu\Theta) & -\mu^2\sin(\mu\Theta) & 0 & 0 \\ -\mu^2\sin(\mu\Theta) & \mu^2\sin(\mu\Theta) & 0 & 0 \end{vmatrix} = 0 \tag{72}$$

from which the characteristic equation is obtained as

$$[2 - 2\mu^2\Theta^2(\alpha_{v_\Theta} + \alpha_{v_{-\Theta}})]\sin(\mu\Theta)\cos(\mu\Theta) = 0. \tag{73}$$

3.4. Asymmetric bifurcation buckling

Each of the three factors of the characteristic Eq. (73) may be equal to zero. The first case is that when the factor $\sin(\mu\Theta) = 0$, its fundamental solution is

$$\mu\Theta = \pi. \tag{74}$$

Substituting Eq. (74) into Eqs. (68)–(71) leads to $E_1 = E_3 = E_4 = 0$ and so the buckling displacement given by Eq. (67) becomes

$$\tilde{v}_{\mathrm{b}} = E_2\sin\left(\frac{\pi\theta}{\Theta}\right), \tag{75}$$

which represents an asymmetric buckling shape.

Substituting Eq. (74) into Eq. (14) leads to the corresponding actual axial compression $\overline{N}$ at buckling as

$$\overline{N} = \frac{\pi^2 EI_x}{(R\Theta)^2} = \frac{\pi^2 EI_x}{(S/2)^2} = N_{EA}. \tag{76}$$

The equation governing the corresponding bifurcation buckling load $\bar{q}_b$ can then be obtained by substituting the solution $\mu\Theta = \pi$ given by Eq. (74) into Eq. (30) as

$$A_3\bar{q}_b^2 + B_3\bar{q}_b + C_3 = 0, \tag{77}$$

with

$$A_3 = 2\pi^2 + 15 + 6\pi^6\left[\frac{\alpha_{v_\Theta} - \alpha_{v_{-\Theta}}}{\pi^2(\alpha_{v_\Theta} + \alpha_{v_{-\Theta}}) - 1}\right]^2, \tag{78}$$

$$B_3 = 12 + 4\pi^2 - \frac{12\pi^4(4\pi^2\alpha_{v_\Theta}\alpha_{v_{-\Theta}} - \alpha_{v_\Theta} - \alpha_{v_{-\Theta}})}{\pi^2(\alpha_{v_\Theta} + \alpha_{v_{-\Theta}}) - 1}, \tag{79}$$

$$C_3 = \frac{12\pi^4}{\lambda^2}(1 + \alpha_{w_\Theta} + \alpha_{w_{-\Theta}}). \tag{80}$$

The corresponding displacement can be obtained by substituting $\mu\Theta = \pi$ into Eq. (25) as

$$\tilde{v} = \frac{\bar{q}\Theta^2}{\pi^2}\left\{\cos(\mu\theta) - 1 + \frac{1}{2}[(\mu\theta)^2 - \pi^2] - \frac{\pi^3(\alpha_{v_\Theta} - \alpha_{v_{-\Theta}})\mu\theta}{\pi^2(\alpha_{v_\Theta} + \alpha_{v_{-\Theta}}) - 1} + \frac{\pi^4(4\pi^2\alpha_{v_\Theta}\alpha_{v_{-\Theta}} - \alpha_{v_\Theta} - \alpha_{v_{-\Theta}})}{\pi^2(\alpha_{v_\Theta} + \alpha_{v_{-\Theta}}) - 1}\right\}. \tag{81}$$

A real solution of Eq. (77), i.e. for the bifurcation buckling load $\bar{q}_b$, exists when

$$B_3^2 - 4A_3C_3 \geqslant 0 \tag{82}$$

from which

$$\lambda \geqslant \lambda_{sb1} = \frac{4\pi^2\sqrt{3A_3(1 + \alpha_{w_\Theta} + \alpha_{w_{-\Theta}})}}{B_3}. \tag{83}$$

Eq. (83) defines the limiting shallowness λ_{sb1} for possible asymmetric bifurcation buckling. When the shallowness of an elastically supported arch is smaller than λ_{sb1}, the arch does not buckle in an asymmetric bifurcation

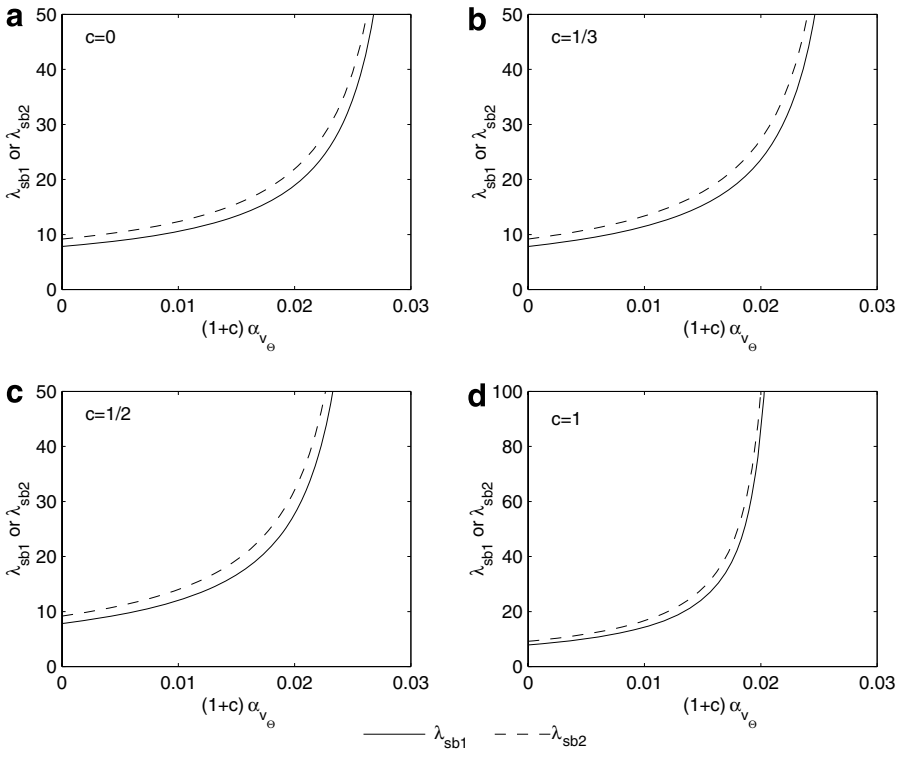

Fig. 4. Variations of limiting shallownesses λ_{sb1} and λ_{sb2} with the flexibility $(1 + c)\alpha_{v_\Theta}$ of elastic radial supports.

mode. Typical variations of limiting shallowness λ_{sb1} with the dimensionless flexibility $(1+c)\alpha_{v_\Theta}$ of the elastic radial supports are shown by the solid line in Fig. 4, where $c = \alpha_{v_{-\Theta}}/\alpha_{v_\Theta}$ is the ratio of flexibilities of elastic radial supports at both ends of an arch, and for convenience the axial supports are assumed to be rigid. It is worth pointing out that when the shallowness λ of an arch is greater than λ_{sb1}, asymmetric bifurcation buckling may occur after the occurrence of snap-through buckling because the displacement given by Eq. (81)

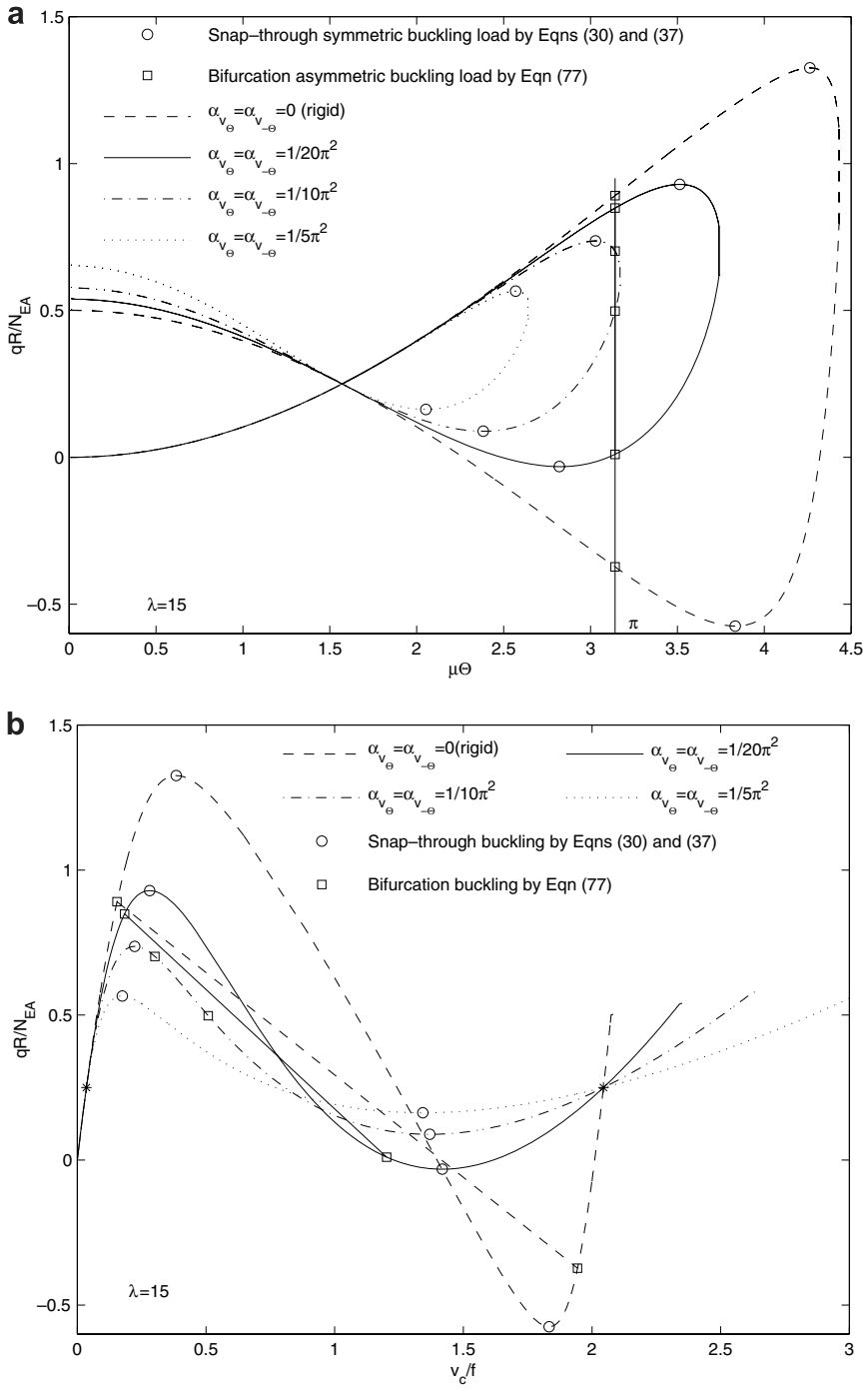

Fig. 5. Nonlinear buckling behaviour of arches with equal elastic radial supports. Variations of dimensionless load $\bar{q}$ with the (a) modified angle $\mu\Theta$ and (b) dimensionless central radial displacement v_c/f.

corresponding to asymmetric bifurcation buckling may be greater than the displacement corresponding to snap-through buckling. A limiting shallowness λ_{sb2} can be used to define a switch between snap-through buckling and bifurcation buckling. The value of the limiting shallowness λ_{sb2} can be found by equating $\bar{q}_{st}$ obtained from Eq. (37) to $\bar{q}_b$ obtained from Eq. (77) at $\mu\Theta = \pi$. The typical variations of the limiting shallowness λ_{sb2} with the dimensionless flexibility $(1+c)\alpha_{v_\Theta}$ of the elastic radial supports are also shown by the dashed line in Fig. 4. It can be seen from Fig. 4 that the values of limiting shallownesses λ_{sb1} and λ_{sb2} vary not only with dimensionless flexibility $(1+c)\alpha_{v_\Theta}$ of the elastic radial supports, but also with the ratio c of the flexibilities of the elastic radial supports. It can be seen that as the dimensionless flexibility $(1+c)\alpha_{v_\Theta}$ increases, the limiting shallownesses λ_{sb1} and λ_{sb2} increase rapidly, which indicates that if the elastic radial supports of an arch are too flexible, buckling of the arch is possible only when it is extremely shallow.

3.5. Effects of flexibility of elastic radial supports

The effects of the flexibility $(1+c)\alpha_{v_\Theta}$ of the elastic radial supports on the nonlinear behaviour of arches can be obtained from Eq. (30), and are shown in Fig. 5 for an arch with equal elastic radial supports of different flexibility at both ends ($c = 1$) and in Fig. 6 for an arch with one rigid and one elastic radial support of different flexibility ($c = 0$). Figs. 5(a) and 6(a) show the variations of the modified axial force parameter $\mu\Theta$ with the dimensionless external load qR/N_{EA}, while Figs. 5(b) and Fig. 6(b) show the variations of the dimensionless central radial displacement v_c/f with the dimensionless external load qR/N_{EA}. It can be seen that the flexibility $(1+c)\alpha_{v_\Theta}$ of the elastic radial supports affects the nonlinear behaviour of an arch significantly. The displacement–load curve and the axial force parameter–load curve for more flexible radial supports ($\alpha_{v_\Theta} = \alpha_{v_{-\Theta}} = 1/5\pi^2$ in Fig. 5 and $\alpha_{v_\Theta} = 1/4.5\pi^2$ and $\alpha_{v_{-\Theta}} = 0$ in Fig. 6) are much lower than those for less flexible radial supports ($\alpha_{v_\Theta} = \alpha_{v_{-\Theta}} = 1/20\pi^2$ in Fig. 5 and $\alpha_{v_\Theta} = 1/20\pi^2$ and $\alpha_{v_{-\Theta}} = 0$ in Fig. 6). The snap-through buckling loads obtained by solving Eqs. (30) and (37) simultaneously and the asymmetric bifurcation buckling loads given by Eq. (77) are also shown in Figs. 5 and 6. It can be seen that the flexibility $(1+c)\alpha_{v_\Theta}$ of the elastic radial supports also affects the buckling mode of an arch. For more flexible elastic radial supports $\alpha_{v_\Theta} = \alpha_{v_{-\Theta}} = 1/5\pi^2$ (Fig. 5) and $\alpha_{v_\Theta} = 1/4.5\pi^2$ and $\alpha_{v_{-\Theta}} = 0$ (Fig. 6), snap-through buckling is the only possible buckling mode. For less flexible elastic radial supports $\alpha_{v_\Theta} = \alpha_{v-\Theta} = 1/20\pi^2$ (Fig. 5) and $\alpha_{v_\Theta} = 1/20\pi^2$ and $\alpha_{v_{-\Theta}} = 0$ (Fig. 6), the buckling load qR/N_{EA} for asymmetric bifurcation buckling, the corresponding axial force parameter $\mu\Theta$, and the corresponding displacement v_c/f are smaller than those for snap-through buckling. Hence, snap-through buckling will generally not occur and asymmetric bifurcation buckling is the dominant mode. For elastic radial supports with the flexibility $\alpha_{v_\Theta} = \alpha_{v-\Theta} = 1/10\pi^2$ (Fig. 5) and $\alpha_{v_\Theta} = 1/6.5\pi^2$ and $\alpha_{v_{-\Theta}} = 0$ (Fig. 6), although the asymmetric bifurcation buckling load qR/N_{EA} is lower than the snap-through buckling load, the axial force parameter $\mu\Theta$ and displacement v_c/f corresponding to asymmetric bifurcation buckling are larger than those corresponding to snap-through buckling. In this case, snap-through buckling occurs first and then asymmetric bifurcation buckling occurs on the descending branch of the curves under displacement control.

The effects of the flexibility of the elastic radial supports are also shown in Fig. 7 as the variations of the dimensionless buckling load qR/N_{EA} with the shallowness λ of an arch. The buckling load of pin-ended arches ($\alpha_{v_\Theta} = \alpha_{v_{-\Theta}} = 0$) are also shown in Fig. 7 for comparison. It can be seen that the buckling loads of the elastically supported arches are lower than those of pin-ended arches. The buckling loads decrease with an increase of the flexibility of the elastic radial supports, particularly for arches with the shallowness $10 \leqslant \lambda \leqslant 40$. The limiting shallowness λ_{sb2} that defines the switch between snap-through and bifurcation buckling modes increases with an increase of the dimensionless flexibility $(1+c)\alpha_{v_\Theta}$ of the elastic radial supports.

3.6. Symmetric buckling load

The factor $\cos(\mu\Theta)$ of the characteristic Eq. (73) may be equal to zero; the fundamental solution of $\cos(\mu\Theta) = 0$ is

$$\mu\Theta = \frac{\pi}{2} \tag{84}$$

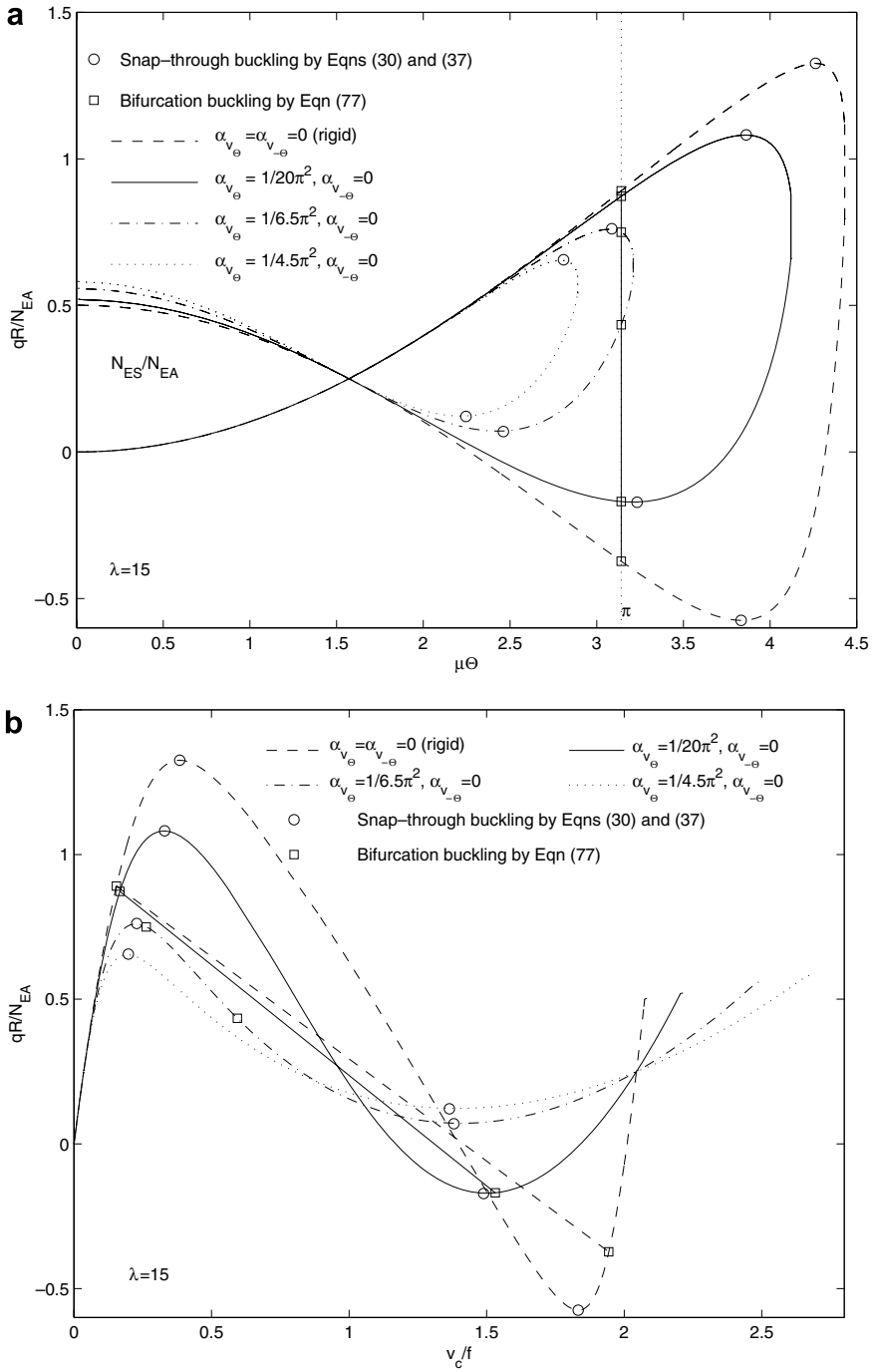

Fig. 6. Nonlinear buckling behaviour of arches with one rigid and one elastic radial support. Variations of dimensionless load $\bar{q}$ with the (a) modified angle $\mu\Theta$ and (b) dimensionless central radial displacement v_c/f.

and substitution of this into Eqs. (68)–(71) leads to $E_2 = E_3 = E_4 = 0$ and so the buckling displacement given by Eq. (67) becomes

$$\tilde{v}_b = E_1 \cos\left(\frac{\pi\theta}{2\Theta}\right), \tag{85}$$

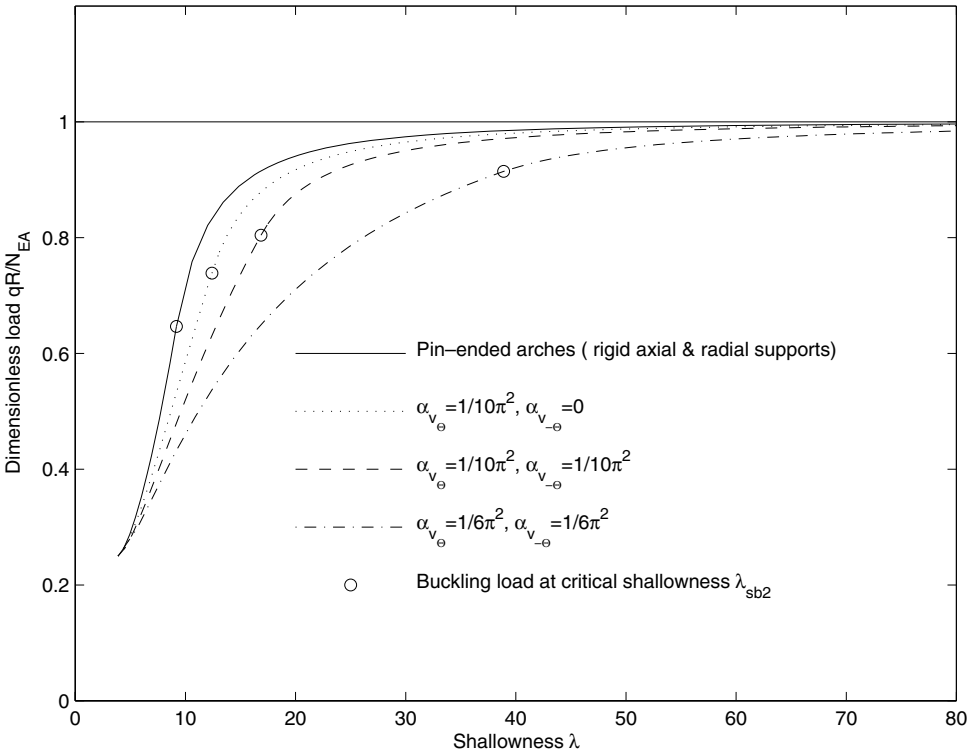

Fig. 7. Effects of elastic radial supports on buckling of arches.

which represents a symmetric buckling shape.

Substituting Eq. (84) into Eq. (14) leads the corresponding actual axial compression $\overline{N}$ at buckling as

$$\overline{N} = \frac{\mu^2 EI_x}{R^2} = \frac{\pi^2 EI_x}{(2R\Theta)^2} = \frac{\pi^2 EI_x}{S^2} = N_{ES}, \tag{86}$$

where N_{ES} is equal to the first mode flexural buckling load of a simply supported column under uniform compression.

The buckling load $\bar{q}$ corresponding to $\mu\Theta = \pi/2$ can be obtained by substituting $\mu\Theta = \pi/2$ into Eq. (30). Because at $\mu\Theta = \pi/2$, $\tan(\pi/2)$ and so the values of A_1 and B_1 given by Eqs. (31) and (32) become infinite, a limit calculation needs to be used to obtain the dimensionless buckling load $\bar{q}$ as

$$\lim_{\mu\Theta\to\pi/2} \bar{q} = \lim_{\mu\Theta\to\pi/2} \frac{\left(-B_1 \pm \sqrt{B_1^2 - 4A_1C_1}\right)}{2A_1} = 0 \tag{87}$$

from which and by considering Eqs. (15) and (86), the symmetric buckling load q can be obtained as

$$qR = \overline{N} = N_{ES} = \frac{\pi^2 EI_x}{S^2}. \tag{88}$$

The displacement $\tilde{v}$ corresponding to the buckling load given by Eq. (88) can be obtained by substituting $\mu\Theta = \pi/2$ into Eq. (25) as

$$\tilde{v} = \frac{16\Theta^2 \cos(\pi\theta/2\Theta)}{\pi^3}\left[1 \mp \sqrt{1 - \frac{\pi^6(1 + \alpha_{w_\Theta} + \alpha_{w_{-\Theta}})}{64\lambda^2}}\right]. \tag{89}$$

Eq. (89) has real solutions only when $\lambda \geqslant \lambda_{sn} = \pi^3/8(1+\alpha_{w_\Theta}+\alpha_{w_{-\Theta}}) \approx 3.88(1+\alpha_{w_\Theta}+\alpha_{w_{-\Theta}})$, where λ_{sn} is a limiting shallowness and when the shallowness $\lambda < \lambda_{sn}$, there is no buckling. When the shallowness $\lambda = \lambda_{sn}$, Eq. (89) produces a unique value of $\tilde{v}$ that corresponds to the buckling load $qR = N_{ES}$ given by Eq. (88) as shown in Fig. 8 for different flexibilities of the elastic radial supports. It can be seen that the flexibility of the elastic radial supports does not affect the value of the limiting shallowness λ_{sn}. This can also be seen in Fig. 7 that $\lambda_{sn} = \pi^3(1+\alpha_{w_\Theta}+\alpha_{w_{-\Theta}})/8$ for different flexibilities of the elastic radial supports. For arches with $\lambda > \lambda_{sn}$, Eq. (89) gives two values of the radial displacement $\tilde{v}$ that correspond to the same load $qR = N_{ES}$. In this case, $\tilde{v}$ and qR define equilibrium configurations, but these equilibrium configurations do not necessarily correspond to a buckling equilibrium as indicated by asterisks in Fig. 9. For these arches ($\lambda > \lambda_{sn}$), snap-through buckling is possible and the buckling load can be obtained by simultaneously solving Eqs. (30) and (37) also as shown in Fig. 9.

3.7. Critical stiffness of radial restraints

When the factor $2-2\mu^2\Theta^2(\alpha_{v_\Theta}+\alpha_{v_{-\Theta}})$ of the characteristic Eq. (73) vanishes, the fundamental solution of $2-2\mu^2\Theta^2(\alpha_{v_\Theta}+\alpha_{v_{-\Theta}})=0$ is

$$\mu\Theta = \eta\pi = \sqrt{\frac{1}{\alpha_{v_\Theta}+\alpha_{v_{-\Theta}}}}. \tag{90}$$

Substituting Eq. (90) into Eq. (14) leads the actual axial compression $\overline{N}$ at the buckling as

$$\overline{N} = \frac{\mu^2 EI_x}{R^2} = \frac{4(\eta\pi)^2 EIx}{S^2} = \frac{4EI_x}{S^2(\alpha_{v_\Theta}+\alpha_{v_{-\Theta}})} = \frac{4EI_x}{S^2(1+c)\alpha_{v_\Theta}}. \tag{91}$$

When the radial supports are sufficiently flexible, $\overline{N}$ given by Eq. (91) is less than N_{ES} given by Eq. (86) and so buckling corresponds to the axial force given in Eq. (91). As the flexibility $(1+c)\alpha_{v_\Theta}$ decreases, $\overline{N}$ given by Eq. (91) increases until $\overline{N} = N_{ES}$. Any further decrease of the flexibility $(1+c)\alpha_{v_\Theta}$ will lead to $\overline{N}$ by Eq. (91) being greater than $\pi^2 EI_x/S^2$, which implies the axial force $\overline{N} = N_{ES}$ given by Eq. (86) governs the buckling. This means that a further decrease of the flexibility of the radial supports will not result in an increase of the symmetric bifurcation buckling load. The flexibility $(1+c)\alpha_{v_\Theta}$ corresponding to N_{ES} is called the critical flexibility of the radial supports. Its value can be obtained by comparing Eq. (91) with Eq. (86), from which $\eta = 1/2$ and the critical flexibility can be obtained from Eq. (90) as

$$(\alpha_{v_\Theta}+\alpha_{v_{-\Theta}})^{cr} = (1+c)\alpha_{v_\Theta}^{cr} = \frac{1}{(\eta\pi)^2} = \frac{4}{\pi^2}. \tag{92}$$

The buckling load $\bar{q}$ corresponding to the solution (90) can be obtained by substituting Eq. (90) into Eq. (30) as

$$\lim_{\alpha_{v_\Theta}(1+c)\to 1/(\eta\pi)^2} \bar{q} = 0 \tag{93}$$

from which and using Eq. (15), the buckling load is then obtained as

$$qR = \overline{N} = \frac{4EI_x}{S^2(1+c)\alpha_{v_\Theta}}, \tag{94}$$

and the corresponding displacement is obtained by substituting Eq. (90) into Eq. (25) as

$$\tilde{v} = \left[\frac{\Theta^2(1-c)^2}{(1+c)^2} + \frac{\Theta\theta(1-c)}{(1+c)}\right]\left[1 \mp \sqrt{1-\frac{2(1+c)(1+\alpha_{w_\Theta}+\alpha_{w_{-\Theta}})}{\lambda^2\alpha(1-c)^2}}\right]. \tag{95}$$

A real value for the displacement $\tilde{v}$ given by Eq. (95) exists only when

$$\lambda \geqslant \lambda_{sn} = \sqrt{\frac{2(1+c)(1+\alpha_{w_\Theta}+\alpha_{w_{-\Theta}})}{\alpha_{v_\Theta}}}\frac{1}{1-c}, \tag{96}$$

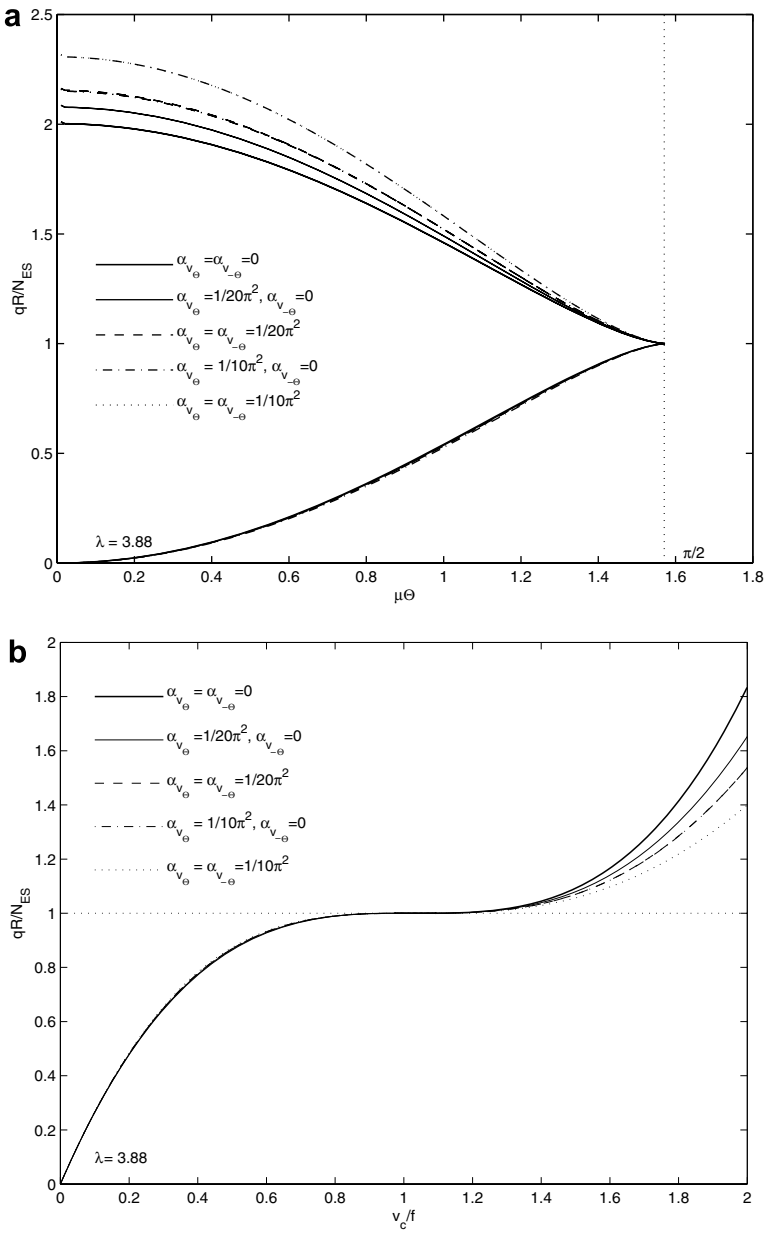

Fig. 8. Nonlinear behaviour at the lowest buckling load. Variations of dimensionless load $\bar{q}$ with the (a) modified angle $\mu\Theta$ and (b) dimensionless central radial displacement v_c/f.

where λ_{sn} is a limiting shallowness. When $\lambda = \lambda_{sn}$, a unique value of the displacement is given by Eq. (95) and the arch may buckle at the load given by Eq. (94) as shown by the broken lines in Fig. 10, where the flexibility of one elastic radial support is $\alpha_{v_\Theta} = 16/\pi^2$ and the other radial support is rigid ($c = 0$), and the limiting shallowness $\lambda_{sn} = 1.11$. When the shallowness λ is smaller than the limiting shallowness λ_{sn} ($\lambda = 0.8 < \lambda_{sn}$), there is no buckling as shown by dotted lines in Fig. 10. When the shallowness $\lambda = 2$ or $3.88 > \lambda_{sn}$, Eq. (95) yields two values of displacements for the same load given by Eq. (94). Although this load and the corresponding two displacements are on the equilibrium path, they do not correspond to a buckling equilibrium as shown by asterisks in Fig. 10. In this case, the arches may buckle in a snap-through mode instead, and the buckling load can be obtained by solving Eqs. (30) and (37) simultaneously, also as shown in Fig. 10.

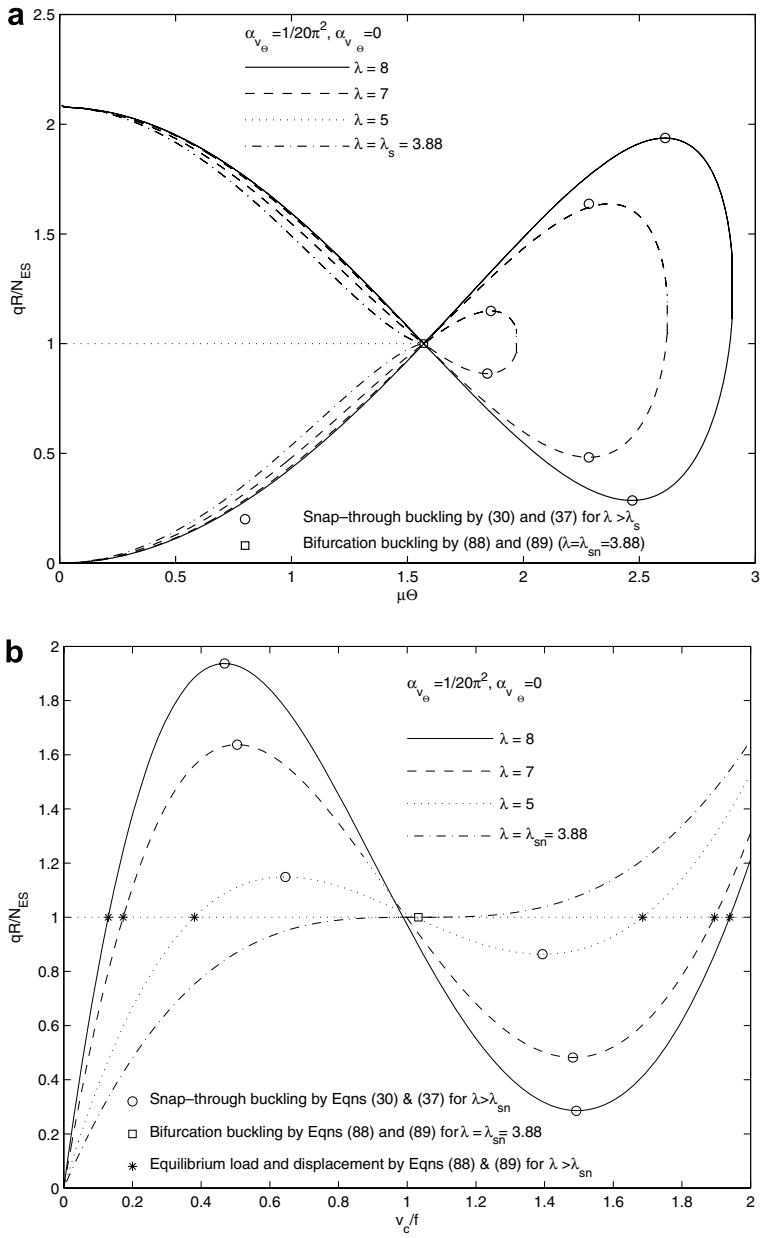

Fig. 9. Symmetric snap-through buckling and bifurcation buckling. Variations of dimensionless load $\bar{q}$ with the (a) modified angle $\mu\Theta$ and (b) dimensionless central radial displacement v_c/f.

For the case of equal elastic radial supports, $c = 1$ and so the limiting shallowness λ_{sn} and the displacement $\tilde{v}$ become infinite, which indicates that when an arch has equal elastic radial supports with flexibility greater than the critical value given by Eq. (92), the arch does not buckle and the arch replicates an elastically supported beam curved in elevation.

3.8. Effects of elastic axial supports

For convenience of comparison in the previous study of the effects of the elastic radial supports, the axial supports were assumed to be rigid ($\alpha_{w_\Theta} = \alpha_{w_{-\Theta}} = 0$). In fact, it can be seen from Eqs. (30), (37), and (77) that

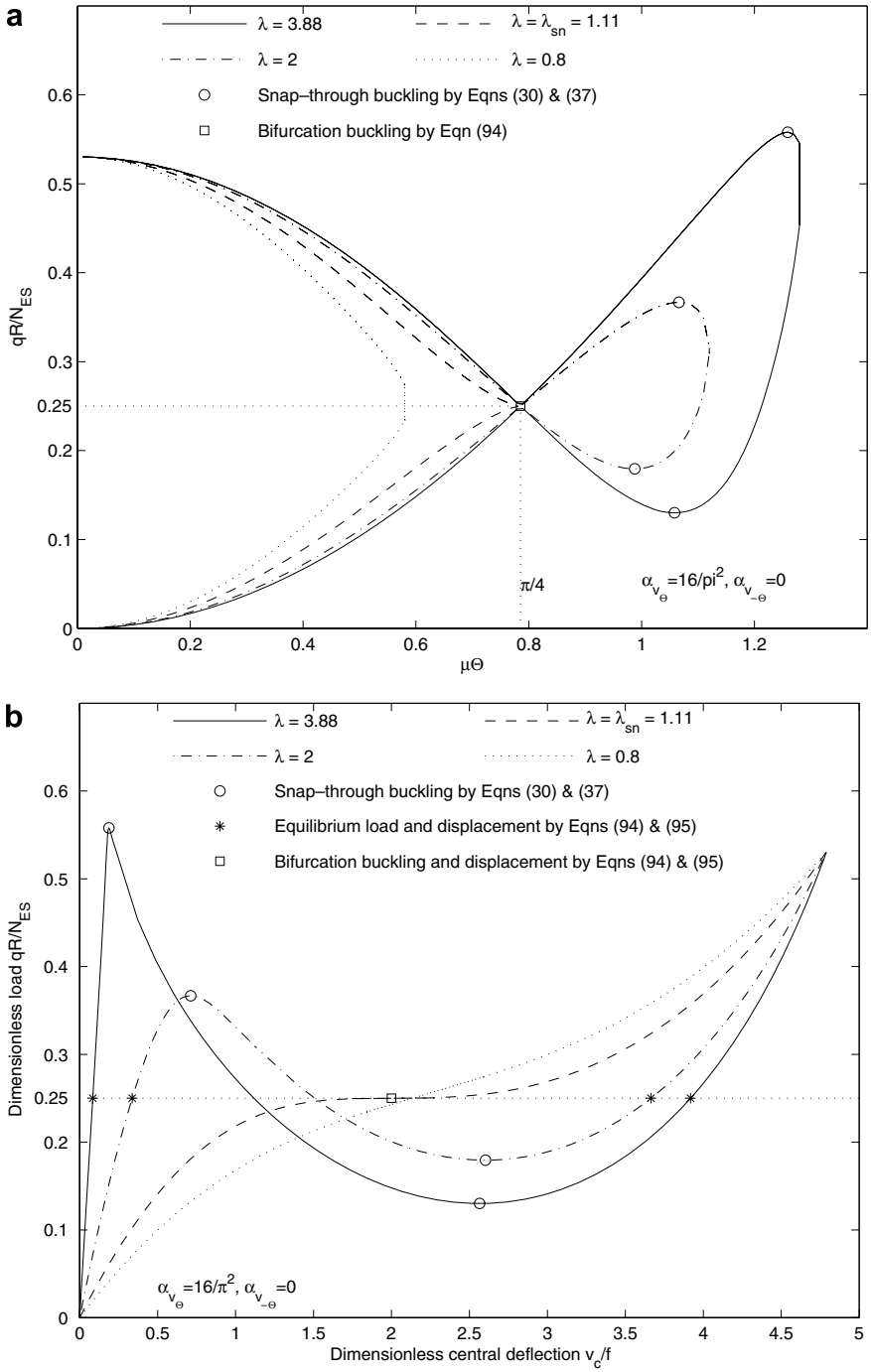

Fig. 10. Nonlinear buckling behaviour of arches with one rigid and one elastic radial support of flexibility larger than the critical value. Variations of dimensionless load $\bar{q}$ with the (a) modified angle $\mu\Theta$ and (b) dimensionless central radial displacement v_c/f.

the flexibility of elastic axial supports may affect the nonlinear behaviour, the snap-through buckling, and bifurcation buckling as well.

The effect of the dimensionless flexibility $(\alpha_{w_\Theta} + \alpha_{w_{-\Theta}})$ of the elastic axial supports on the limiting shallowness that distinguishes between the buckling modes is shown in Fig. 11 as variations of the shallownesses λ_{sn}, λ_{sb1}, and λ_{sb2} with the flexibility $(\alpha_{w_\Theta} + \alpha_{w_{-\Theta}})$ of the elastic axial supports. It can be seen that with an increase

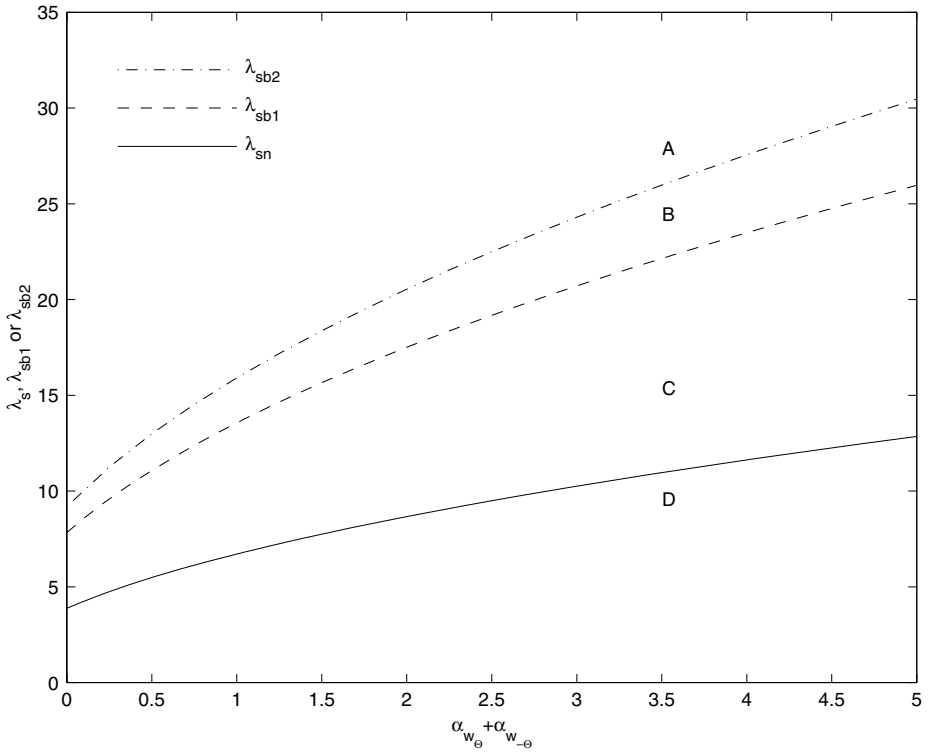

Fig. 11. Effects of elastic axial supports on limiting shallownesses of arches λ_{sb1}, λ_{sb2} and λ_{sn}.

of the flexibility $(\alpha_{w_\Theta} + \alpha_{w_{-\Theta}})$, the limiting shallownesses λ_{sn}, λ_{sb1}, and λ_{sb2} increase. When the shallowness λ of an arch is in region A of Fig. 11, the arch may buckle in an asymmetric bifurcation mode; for λ in region B, the arch may buckle in a symmetric snap-through or an asymmetric bifurcation buckling mode; for λ in region C, the arch may buckle only in a symmetric snap-through mode; and for λ in region D, the arch does not buckle. When the flexibility of the elastic axial supports approaches to infinity, the corresponding limiting value of the shallowness λ approaches infinity. In this case, the arch becomes an elastically supported beam curved in elevation.

Fig. 12 shows the variation of the dimensionless buckling load qR/N_{EA} with the shallowness λ for three groups of arches with elastic axial supports, where for the convenience of comparison, the radial supports are assumed to be rigid. The flexibility of the elastic axial supports of the three groups of arches are $\alpha_{w_\Theta} = \alpha_{w_{-\Theta}} = 0.5$, 1.5, and 2.5 respectively. For comparison, the results of pin-ended arches $(\alpha_{w_\Theta} = \alpha_{w_{-\Theta}} = 0)$ are also shown in Fig. 12. It can be seen that as the flexibility of the elastic axial supports increases, i.e. the stiffness of the elastic axial supports decreases, the buckling loads of the arches decreases. It can also be seen from Fig. 12 that the flexibility $(\alpha_{w_\Theta} + \alpha_{w_{-\Theta}})$ of the elastic axial supports also affects the limiting shallowness λ_{sn}. As the flexibility $(\alpha_{w_\Theta} + \alpha_{w_{-\Theta}})$ increases, the limiting shallowness λ_{sn} increases. This is different from the case of the elastic radial supports. When the flexibility of elastic radial supports is lower than the critical flexibility given by Eq. (92), the flexibility $(1 + c)\alpha_{v_\Theta}$ does not affect the limiting shallowness λ_{sn} as shown in Fig. 7.

3.9. Summary

There are two important critical parameters that govern the buckling mode of an elastically supported shallow arch: the critical flexibility of its radial elastic supports and the limiting shallownesses of the arch.

From Eq. (92), the critical flexibility $\alpha^{cr}_{v_\Theta}$ of the elastic radial supports is given by $\alpha^{cr}_{v_\Theta} = 4/[(1 + c)\pi^2]$. When the flexibility $\alpha^{cr}_{v_\Theta}$ of the radial elastic supports is less than the critical value $4/[(1 + c)\pi^2]$, the buckling mode of

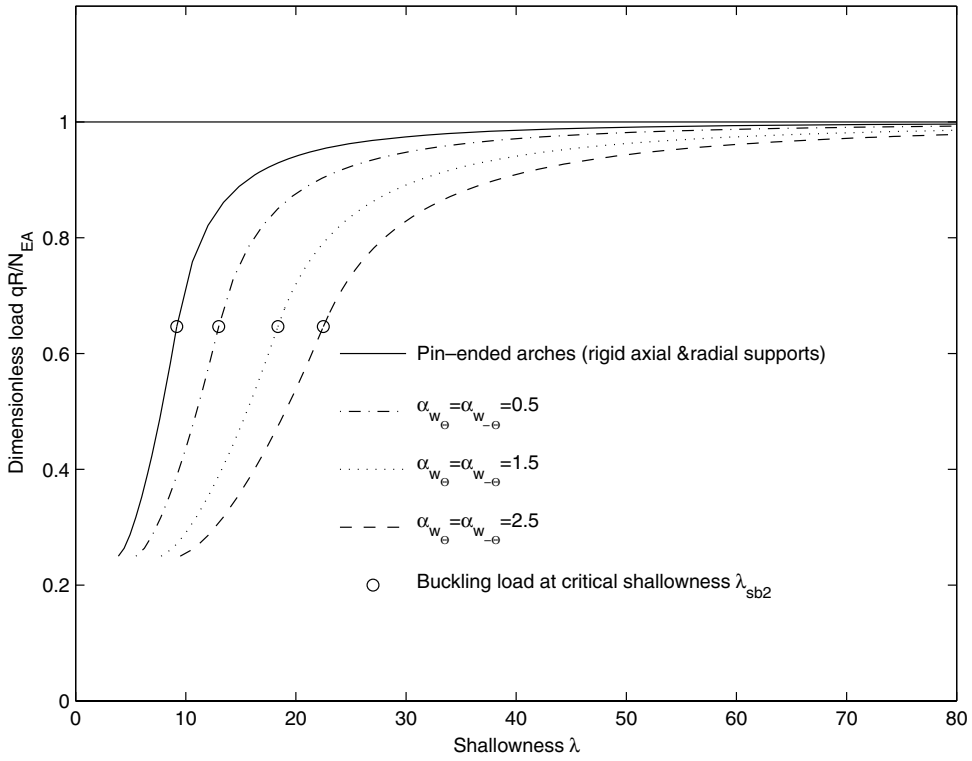

Fig. 12. Effects of elastic axial supports on buckling of arches.

an arch depends on its shallowness λ. If the shallowness is less than the critical value $\lambda_{sn} = 3.88(1 + \alpha_{w_\Theta} + \alpha_{w_{-\Theta}})$, i.e. $\lambda < \lambda_{sn}$, there is no buckling for the arch. If the shallowness is equal to the critical value λ_s, the arch buckles in a symmetric bifurcation mode. If the shallowness is greater than the critical value λ_s, but lower than the critical value λ_{sb1} given by Eq. (83), the snap-through buckling load given by Eqs. (30) and (37) is lower than the asymmetric bifurcation buckling load given by Eq. (77) and the arch buckles in a snap-through mode. If the shallowness is greater than the critical value λ_{sb2} given in Fig. 6, the snap-through buckling load given by Eqs. (30) and (37) is higher than the asymmetric bifurcation buckling load given by Eq. (77) and the arch buckles in an asymmetric bifurcation mode. If the shallowness is greater than the critical value λ_{sb1} given by Eq. (83), but lower than the critical value λ_{sb2} given in Fig. 6, although the snap-through buckling load given by Eqs. (30) and (37) is higher than the asymmetric bifurcation buckling load given by Eq. (77), the displacement corresponding to the snap-through buckling is smaller than that corresponding to the asymmetric buckling and so the arch buckles first in a snap-through mode and then in an asymmetric buckling mode.

When the flexibility of the radial elastic supports is greater than the critical value $4/[(1 + c)\pi^2]$, the behaviour of arches with unequal radial elastic supports is different from that of arches with equal radial elastic supports. For arches with unequal radial elastic supports, the critical value λ_{ss} that defines the switch between no buckling and symmetric buckling is given by Eq. (96). When the shallowness is less than λ_{ss}, the arch does not buckle. When the shallowness is equal to λ_{ss}, the arch buckles in a symmetric mode and the buckling load is given by Eq. (94). When the shallowness is greater than λ_{ss}, the arch buckles in a snap-through mode and buckling load is given by the solution of Eqs. (30) and (37). The behaviour of arches with equal radial elastic supports is similar to that of a beam curved in elevation, and the arches do not buckle.

4. Comparisons with FE results

The analytical solution for the bifurcation buckling obtained from Eq. (77) and the solution for snap-through buckling obtained by simultaneously solving Eqs. (30) and (37) for arches with end elastic radial

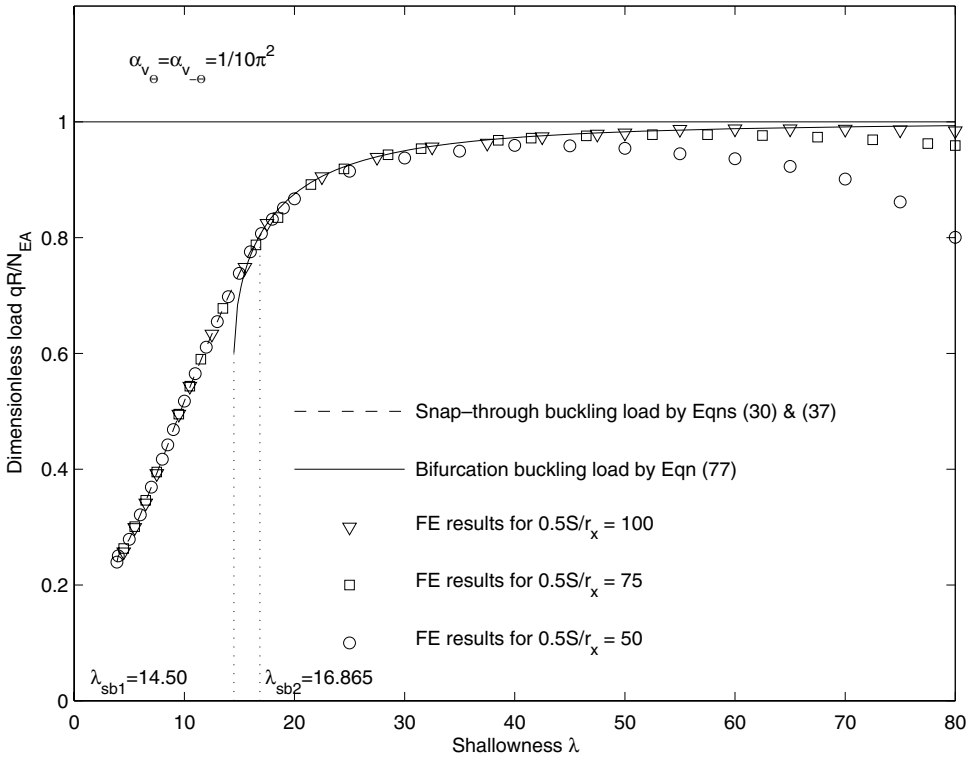

Fig. 13. Comparison with FE buckling results.

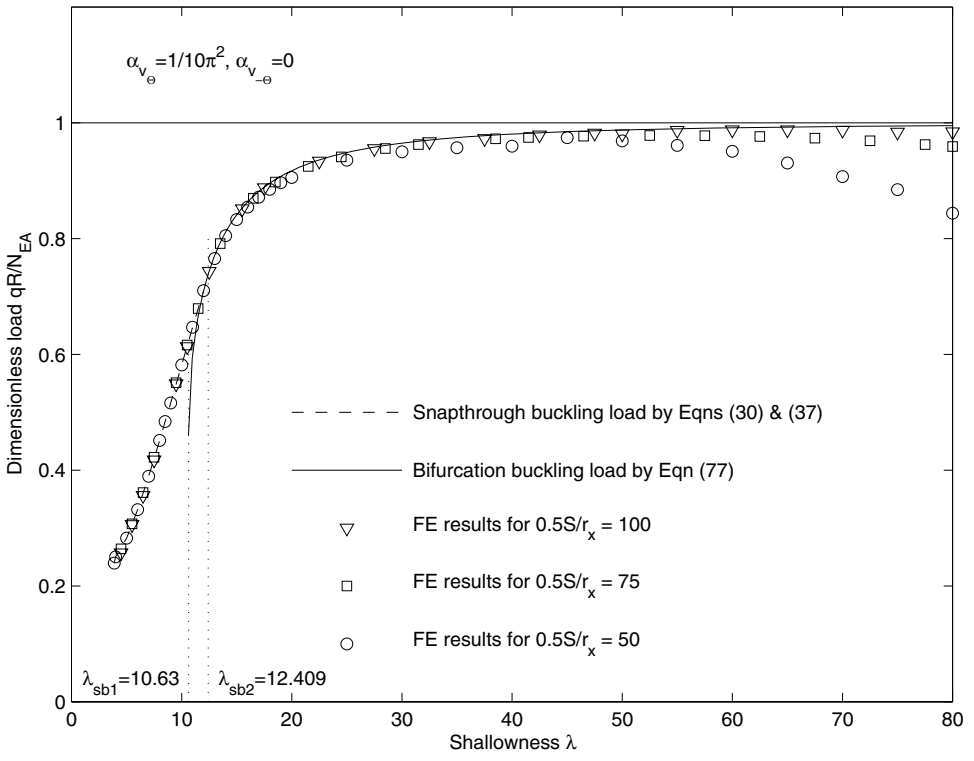

Fig. 14. Comparison with FE buckling results.

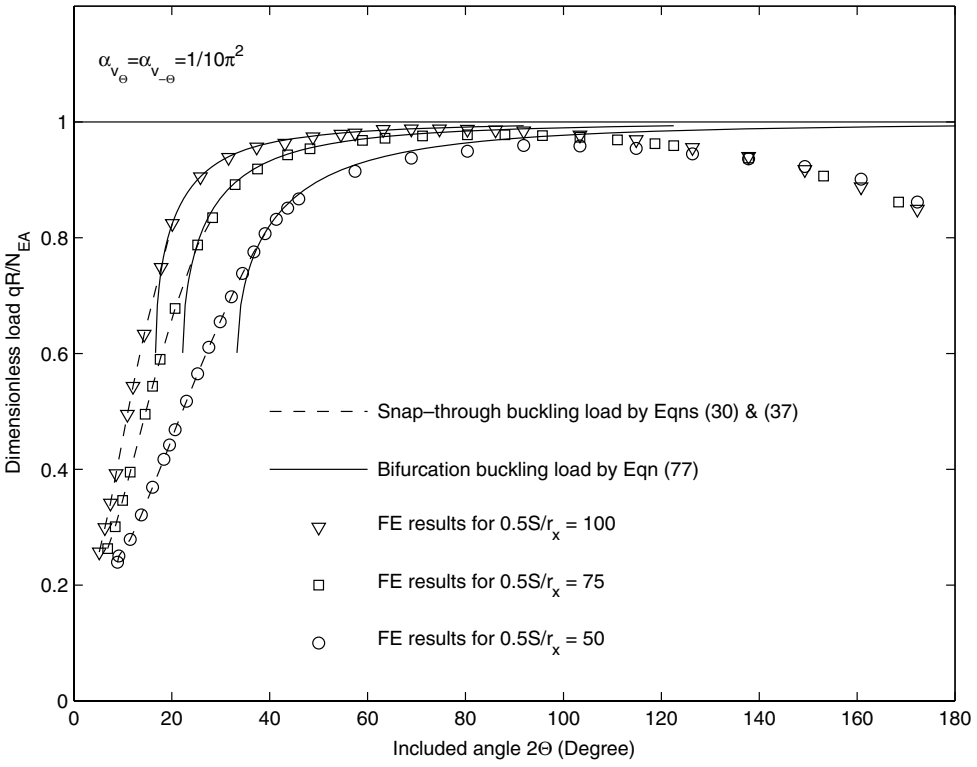

Fig. 15. Comparison with FE buckling results ($\alpha_{v_\Theta}=\alpha_{v_{-\Theta}}=1/10\pi^2$).

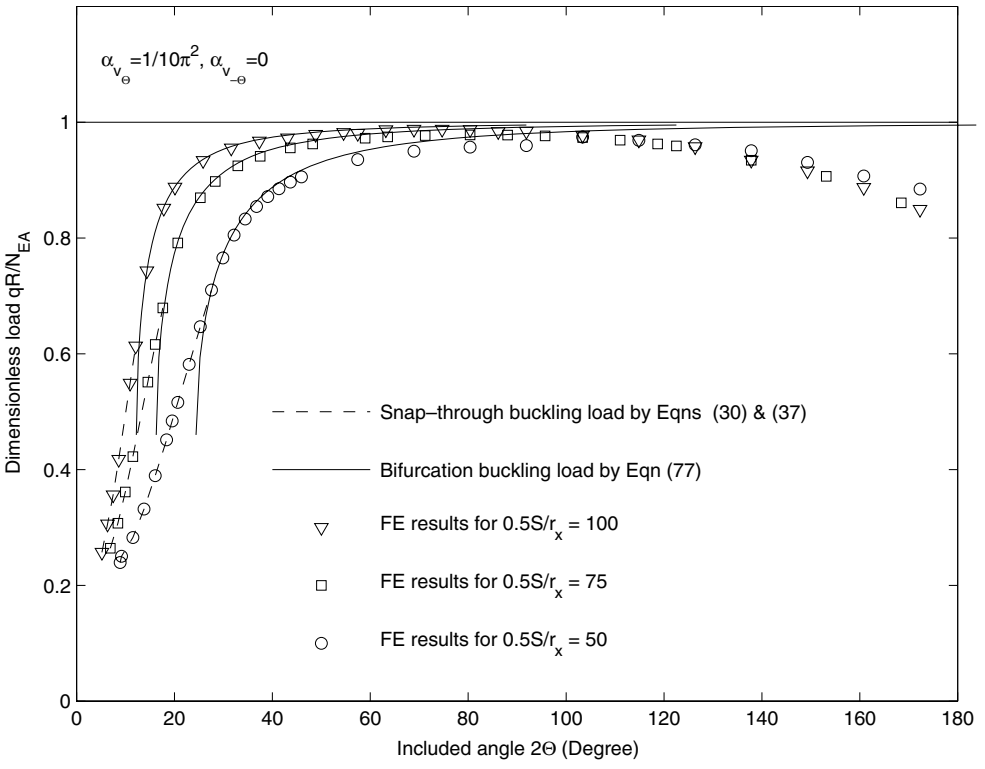

Fig. 16. Comparison with FE buckling results ($\alpha_{v_\Theta}=1/10\pi^2,\ \alpha_{v_{-\Theta}}=0$).

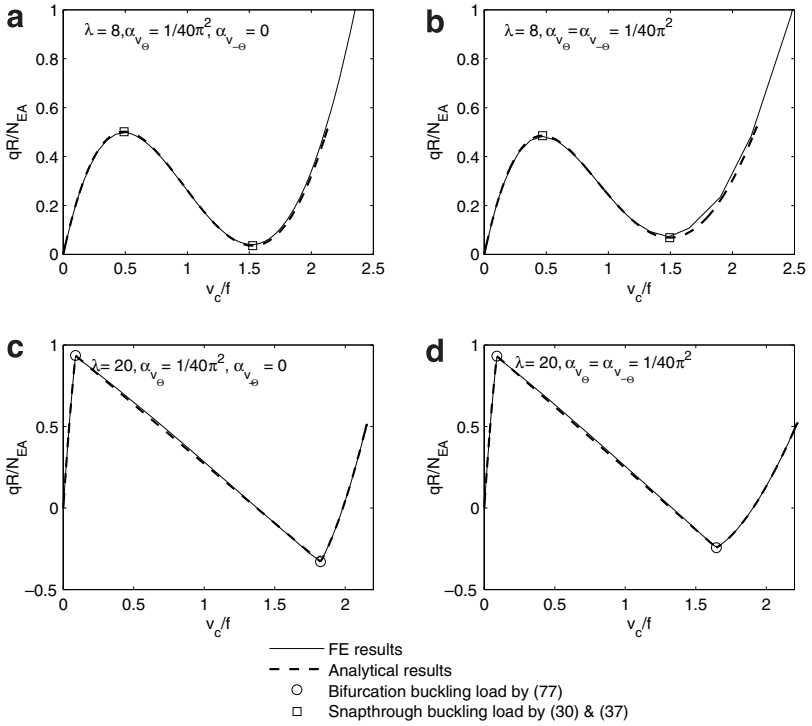

Fig. 17. Comparison with FE nonlinear results.

supports are compared with finite element (FE) predictions in Figs. 13 and 14 as variations of the dimensionless load qR/N_{EA} with the shallowness λ of arches, and in Figs. 15 and 16 as variations of the dimensionless load qR/N_{EA} with the included angle 2Θ of arches. The arches in Figs. 13 and 15 have equal elastic radial supports of flexibility $\alpha_{v_\Theta} = \alpha_{v_{-\Theta}} = 1/10\pi^2$ while the arches in Figs. 14 and 16 have one rigid ($\alpha_{v_{-\Theta}} = 0$) and one elastic ($\alpha_{v_\Theta} = 1/10\pi^2$) radial support. The FE results were obtained by FE package ABAQUS (1998) and by the finite restrained curved-beam element developed by Pi and Trahair (1998). In the ABAQUS analysis, a beam element and spring element were used to model the arches and the elastic supports respectively. In the FE analysis, three cases: $I_x = 6.61 \times 10^7\ \text{mm}^4$ and $A = 5.54 \times 10^3\ \text{mm}^2$, $I_x = 7.44 \times 10^7\ \text{mm}^4$ and $A = 3.86 \times 10^3\ \text{mm}^2$, and $I_x = 104\ \text{mm}^4$ and $A = 50\ \text{mm}^2$ were studied. The Young' modulus of elasticity is assumed to be equal to $E = 200{,}000$ MPa. The results of ABAQUS are identical to those of Pi and Trahair. It can be seen from Figs. 13–16 that the solutions of Eq. (77) for asymmetric bifurcation buckling loads and solutions of Eqs. (30) and (37) for snap-through buckling loads agree very well with the FE results for shallow arches, particularly for arches with an included angle $2\Theta \leqslant 90°$.

The nonlinear behaviour obtained from Eq. (30) for arches with elastic radial supports are compared with the FE results in Fig. 17. It can be seen that they agree with each other extremely well. For the arches with shallowness $\lambda = 8$, snap-through buckling governs and the buckling loads obtained from Eqs. (30) and (37) coincide with the FE results, as shown in Fig. 17(a) and (b). For the arches with shallowness $\lambda = 20$, asymmetric bifurcation buckling is dominant and the buckling loads given by Eq. (77) are the same as FE results, as shown in Fig. 17(c) and (d).

5. Conclusions

This paper has studied the in-plane nonlinear elastic behaviour and stability of elastically supported shallow circular arches that are subjected to a radial load uniformly distributed around the arch axis. A virtual work formulation produced analytical solutions for the nonlinear analysis of elastically supported shallow arches including nonlinear snap-through and bifurcation buckling and postbuckling. The closed form solutions for

the asymmetric bifurcation buckling load and for the snap-through buckling load have been obtained. Comparisons with FE predictions have shown that the solution for nonlinear analysis predicts the nonlinear behaviour of elastically supported arches correctly, and that solutions for the asymmetric bifurcation buckling and snap-through buckling loads are similarly correct.

It has been found that the effects of the elastic supports on the nonlinear behaviour and buckling loads of an arch are significant. In general, as the flexibilities of the elastic supports of an arch increase, the buckling load of the arch decreases. The flexibilities of the elastic supports also have significant effects on the buckling modes of an arch. The criteria for the classification of different modes of fundamental buckling behaviour have been established. There are four important parameters that govern the buckling mode and load: the critical flexibility $\alpha_{v_\Theta}^{\mathrm{cr}}$ of the elastic supports of an arch, and the three limiting shallownesses λ_{sn}, λ_{sb1} and λ_{sb2} of the arch. The critical flexibility of elastic radial supports is found to be equal to $\alpha_{v_\Theta}^{\mathrm{cr}} = 4/[(1+c)\pi^2]$. The relationships of limiting shallownesses λ_{sn}, λ_{sb1} and λ_{sb2} have been established.

The effect of the flexibility $(\alpha_{w_\Theta} + \alpha_{w_{-\Theta}})$ of elastic axial supports on the limiting shallowness between buckling modes is also important. The limiting shallownesses λ_{sn}, λ_{sb1}, and λ_{sb2} increase with an increase of the flexibility $(\alpha_{w_\Theta} + \alpha_{w_{-\Theta}})$. The flexibility of the elastic axial supports also affects the buckling loads significantly. As the flexibility of the elastic axial supports increases, i.e. the stiffness of the axial supports decreases, the buckling loads of arches decrease, particularly for arches with shallowness $\lambda < 50$. When the flexibility replicates very large, the arch replicates an elastically supported beam curved in elevation.

Acknowledgements

This work has been supported by the Australian Research Council through Discovery Projects awarded to authors and by a Federation Fellowship awarded to the second author.

References

ABAQUS Standard User's Manual version 5.8. 1998. Hibbit, Karlsson and Sorensen Inc., Abaqus, Pawtucket, Rhode Island.

Bradford, M.A., Uy, B., Pi, Y.-L., 2002. In-plane elastic stability of arches under a central concentrated load. Journal of Engineering Mechanics ASCE 128 (7), 710–719.

Bradford, M.A., Pi, Y.-L., Wang, T., Gilbert, R.I., 2005. In-plane buckling of arches with rotational end restraints. Research Report, The University of New South Wales, Sydney, NSW, Australia.

Dickie, J.F., Broughton, P., 1971. Stability criteria for shallow arches. Journal of the Engineering Mechanics Division ASCE 97 (EM3), 951–965.

Dym, C.L., 1973. Bifurcation analyses for shallow arches. Journal of the Engineering Mechanics Division ASCE 99 (EM2), 287–301.

Fung, Y.C., Kaplan, A., 1952. Buckling of low arches of curved beams of small curvature. NACA TN, 2840.

Gjelsvik, A., Bodner, S.R., 1962. Energy criterion and snap-through buckling of arches. Journal of the Engineering Mechanics Division ASCE 88 (EM5), 87–134.

Kyriakides, S., Arseculeratne, R., 1993. Propagating instabilities in long shallow panels. Journal of Engineering Mechanics ASCE 119 (3), 570–583.

Pi, Y.-L., Trahair, N.S., 1998. Non-linear buckling and postbuckling of elastic arches. Engineering Structures 20 (7), 571–579.

Pi, Y.-L., Bradford, M.A., Uy, B., 2002. In-plane stability of arches. International Journal of Solids and Structures 39, 105–125.

Pi, Y.-L., Bradford, M.A., Tin-Loi, F., 2006. Nonlinear analysis of rotationally restrained pin-ended arches. First California Conference on Recent Advance in Engineering Mechanics, Fullerton, CA, USA, pp. 126–131.

Power, T.L., Kyriakides, S., 1994. Localization and propagation of instabilities in long shallow panels under external pressure. Journal of Applied Mechanics ASME 61 (4), 755–763.

Schreyer, H.L., Masur, E.F., 1966. Buckling of shallow arches. Journal of the Engineering Mechanics Division ASCE 92 (EM4), 1–17.

Simites, G.J., 1976. An Introduction to the Elastic Stability of Structures. Prentice-Hall, Englewood Cliffs, NJ, USA.

Timoshenko, S., Gere, J.M., 1961. Theory of Elastic Stability. McGraw-Hill, New York, USA.

Trahair, N.S., Bradford, M.A., Nethercot, D.A., 2001. The Behaviour and Design of Steel Structures to BS5950, 3rd ed. E&FN Spon, London.